



UvA-DARE (Digital Academic Repository)

Rhodium Complexes in P-H Bond Activation Reactions

Varela-Izquierdo, V.; Geer, A.M.; de Bruin, B.; López, J.A.; Ciriano, M.A.; Tejel, C.

DOI

[10.1002/chem.201903981](https://doi.org/10.1002/chem.201903981)

Publication date

2019

Document Version

Final published version

Published in

Chemistry-A European Journal

License

Article 25fa Dutch Copyright Act

[Link to publication](#)

Citation for published version (APA):

Varela-Izquierdo, V., Geer, A. M., de Bruin, B., López, J. A., Ciriano, M. A., & Tejel, C. (2019). Rhodium Complexes in P-H Bond Activation Reactions. *Chemistry-A European Journal*, 25(69), 15915-15928. <https://doi.org/10.1002/chem.201903981>

General rights

It is not permitted to download or to forward/distribute the text or part of it without the consent of the author(s) and/or copyright holder(s), other than for strictly personal, individual use, unless the work is under an open content license (like Creative Commons).

Disclaimer/Complaints regulations

If you believe that digital publication of certain material infringes any of your rights or (privacy) interests, please let the Library know, stating your reasons. In case of a legitimate complaint, the Library will make the material inaccessible and/or remove it from the website. Please Ask the Library: <https://uba.uva.nl/en/contact>, or a letter to: Library of the University of Amsterdam, Secretariat, Singel 425, 1012 WP Amsterdam, The Netherlands. You will be contacted as soon as possible.

P–H activation

Rhodium Complexes in P–H Bond Activation Reactions

V́ctor Varela-Izquierdo,^[a] Ana M. Geer,^{*[b]} Bas de Bruin,^[c] Joś A. Ĺpez,^[a] Miguel A. Ciriano,^[a] and Cristina Tejel^{*[a]}

Abstract: The feasibility of oxidative addition of the P–H bond of PHPh₂ to a series of rhodium complexes to give mononuclear hydrido-phosphanido complexes has been analyzed. Three main scenarios have been found depending on the nature of the L ligand added to [Rh(Tp)(C₂H₄)(PHPh₂)] (Tp = hydridotris(pyrazolyl)borate): i) clean and quantitative reactions to terminal hydrido-phosphanido complexes [RhTp(H)(PPh₂)(L)] (L = PMe₃, PMe₂Ph and PHPh₂), ii) equilibria between Rh^I and Rh^{III} species: [RhTp(H)(PPh₂)(L)] ⇌ [RhTp(PHPh₂)(L)] (L = PMePh₂, PPh₃) and iii) a simple ethylene replacement to give the rhodium(I) complexes [Rh(κ²-Tp)(L)(PHPh₂)] (L = NHCs-type ligands). The position of the P–H oxidative addition–reductive elimination

equilibrium is mainly determined by sterics influencing the entropy contribution of the reaction. When ethylene was used as a ligand, the unique rhodaphosphacyclobutane complex [Rh(Tp)(η¹-Et)(κ^{C-P}-CH₂CH₂PPh₂)] was obtained. DFT calculations revealed that the reaction proceeds through the rate limiting oxidative addition of the P–H bond, followed by a low-barrier sequence of reaction steps involving ethylene insertion into the Rh–H and Rh–P bonds. In addition, oxidative addition of the P–H bond in OPHPh₂ to [Rh(Tp)(C₂H₄)(PHPh₂)] gave the related hydride complex [RhTp(H)(PHPh₂)(POPh₂)], but ethyl complexes resulted from hydride insertion into the Rh–ethylene bond in the reaction with [Rh(Tp)(C₂H₄)₂].

Introduction

P–H bond activation at a single metal center is a critical step in metal-catalyzed transformations involving the formation of P–C and P–P bonds, such as hydrophosphanation, hydrophosphonylation, dehydrocoupling, and polymerization reactions.^[1] In this reaction, the P–H bond transforms into a terminal phosphanido ligand (M–P) thus enhancing its nucleophilic character and consequently its reactivity.^[2]

Among the different approaches to this reaction, one of the most popular involves proton transfer from phosphanes or phosphane oxides to an internal base, that is, a proton acceptor group coordinated to the metal. Relevant examples include protonolysis at alkyl,^[3] and acetate palladium complexes,^[4]

nickel silanolates^[5] and silylamides,^[6] and iron complexes with an Fe–CH₂SiMe₃ motif.^[7] In addition, metals with formal d⁰ electron count such as lanthanides, early transition metals and some actinides engage in σ-bond metathesis as reported for complexes with alkyls,^[8] silylamides,^[9] amides,^[10] and more recently alkoxy groups.^[11]


Moreover, P–H bond activation through metal-ligand cooperation has been recently reported for ruthenium and iridium complexes bearing carbene-type ligands,^[12] whereas chelated assisted P–H bond cleavage has been described for diphosphane-phosphane oxides,^[13] and diphosphane-phosphane compounds,^[14] which results in a phosphanido functionality embedded within a tripodal ligand.

Another interesting methodology that does not require any previous functionalization of the metal center is the oxidative addition reaction, that is, insertion of the metal into a P–H bond, which eventually results in hydrido-phosphanido compounds. However, isolated complexes from such reactions have only been reported in a few instances. As a matter of fact, pioneering work from Schunn^[15] and Ebsworth,^[16] showed the preparation of iridium(III) complexes derived from the oxidative addition of PH₃, whereas diphenylphosphane has been successfully added to iridium(I) complexes only recently.^[17] Moreover, tri-coordinated complexes of platinum(0)^[18] and nickel(0)^[19] react with secondary phosphanes to render mononuclear complexes with a H–M–PR₂ moiety. However, a similar reaction with a related nickel(I) complex bearing a β-diketiminato ancillary ligand stops at the coordination level, simply leading to [Ni(nacnac)(PHPh₂)].^[20] Furthermore, the strong influence of the ancillary ligands in the course of the reactions is

[a] V. Varela-Izquierdo, Dr. J. A. Ĺpez, Prof. Dr. M. A. Ciriano, Dr. C. Tejel
Departamento de Qúmica Inorgánica
Instituto de Síntesis Químicas Catalíticas Homogénea (ISQCH)
CSIC-Universidad de Zaragoza
Pedro Cerbuna 12, 50009 Zaragoza (Spain)
E-mail: ctejel@unizar.es

[b] Dr. A. M. Geer
Department of Chemistry
University of Virginia
Charlottesville, Virginia 22904 (USA)
E-mail: ag3kj@virginia.edu

[c] Prof. Dr. B. de Bruin
University of Amsterdam
Van 't Hoff Institute for Molecular Sciences
Science park 904, 1098 XH Amsterdam (The Netherlands)

 Supporting information and the ORCID identification number(s) for the author(s) of this article can be found under:
<https://doi.org/10.1002/chem.201903981>.

evidenced by the reaction of $[\text{Pt}(\text{PEt}_3)_3]$ with PPh_2 , which gives di- and tri-nuclear hydrido-complexes with phosphanido bridging ligands.^[21] In these circumstances, the reactivity of the phosphanido ligand is considerably reduced because of the lack of lone electron pairs on the phosphorus atom. This undesirable situation can be avoided by using bulky ligands, as observed in the reaction of $[\text{Co}(\text{dtbpe})(\text{C}_2\text{H}_4)]$ ($\text{dtbpe} = 1,2\text{-bis}(\text{di-}t\text{-tert-butylphosphano})\text{ethane}$) with 2,6-dimesitylphenylphosphane (DmpPH_2), which gives $[\text{Co}(\text{dtbpe})(\text{H})(\text{PHDmp})]$.^[22]

Hydrido-phosphanido complexes of early and middle transition metals have also been prepared from oxidative addition reactions of the coordinatively and electronically unsaturated complex $[\text{Ta}(\text{tBu}_3\text{SiO})_3]$,^[23] and also from electronically saturated complexes $[\text{Mo}(\text{Cp}^*)(\text{Cl})(\text{N}_2)(\text{PMe}_3)_2]$,^[24] and $[\text{W}(\text{dppe})_2(\text{N}_2)_2]$ ^[25] with HPPH_2 . The latter require light irradiation to dissociate dinitrogen and thus generate the required coordination vacancy.

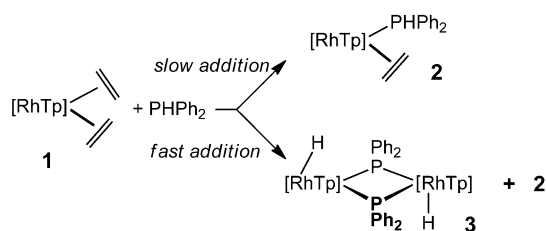
There are few examples of P–H bond activation with rhodium complexes. Particularly pertinent to the present work are the rhodium(III) hydrido-phosphanido intermediates observed by Tilley^[26] in the synthesis of dinuclear bis(phosphanido) bridged complexes and a rhodium(V) bis(hydrido-phosphanido) complex proposed by Brookhart in the catalytic dehydrocoupling of secondary phosphanes.^[27] More recently, Grützmacher reported a terminal rhodium(I)-phosphanido complex with a bulky tetradentate ligand, which contains an unusually long Rh–P bond,^[28] whereas we have isolated mononuclear hydrido-phosphanido rhodium complexes and demonstrated that they are intermediates in catalytic hydrophosphanation and dehydrocoupling reactions.^[29]

In this paper we showcase the feasibility for the oxidative addition reaction of the P–H bond of PPh_2 and OPHP_2 to a series of rhodium complexes that give cleanly new mononuclear hydrido-phosphanido complexes, a rhodaphosphacyclobutane complex or ethyl complexes depending on the ancillary ligands and the reaction conditions. Some clues to account for the different reactivity observed, supported by DFT studies are also provided.

Results and Discussion

Reactions with PMe_3 , PMe_2Ph and PPh_2

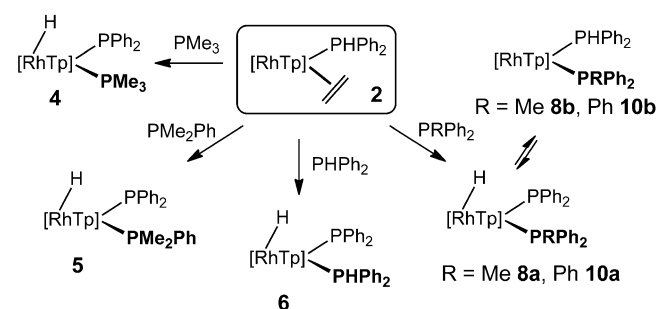
We have previously reported that upon addition of diphenylphosphane to $[\text{Rh}(\text{Tp})(\text{C}_2\text{H}_4)_2]$ (**1**; Tp = hydridotris(pyrazolyl)borate) one ethylene ligand is replaced to give $[\text{Rh}(\text{Tp})(\text{C}_2\text{H}_4)(\text{PPh}_2)]$ (**2**), which was isolated as a yellow microcrystalline solid in excellent yield (Scheme 1).^[29] Complex **2** was



Scheme 1. Reaction of **1** with PPh_2 .

fully characterized as a species with TBPY-5 geometry with a non-rotating ethylene at the equatorial position. Slow addition of PPh_2 under vigorous stirring is required to obtain pure samples of complex **2**; otherwise this compound is contaminated with variable amounts of the dinuclear complex $[\{(\text{Tp})(\text{H})\text{Rh}(\mu\text{-PPh}_2)\}_2]$ (**3**) (Scheme 1).

Addition of P-donor ligands such as PMe_3 , PMe_2Ph , and even PPh_2 to **2** promotes the oxidative addition of the P–H bond to give the hydrido-phosphanido complexes $[\text{Rh}(\text{Tp})(\text{H})(\text{L})(\text{PPh}_2)]$ ($\text{L} = \text{PMe}_3$, **4**, PMe_2Ph , **5**, and PPh_2 , **6**). These reactions were found to be immediate and quantitative by ^1H and $^{31}\text{P}\{^1\text{H}\}$ NMR spectroscopy,^[29] and complexes **5–6** have now been isolated as yellow microcrystalline solids after workup (Scheme 2).



Scheme 2. Synthesis of complexes **4–6**, **8** and **10** through P–H bond activation reactions.

These complexes represent the first isolated terminal phosphanido rhodium complexes resulting from the formal oxidative addition of a P–H bond to a rhodium center. According to the formulation, complex **6** can be directly prepared by adding two molar equivalents of PPh_2 to the bis(ethylene) complex **1**.

Complexes **4** and **5** were characterized in solution as single static species by the signal of the hydride ligand at high field ($\delta = -15.62$ and -15.44 ppm, respectively) in their ^1H NMR spectra and two doublets of doublets for the two inequivalent phosphorus atoms in the $^{31}\text{P}\{^1\text{H}\}$ NMR spectra. Interestingly, the values of $J(\text{P},\text{Rh})$ for the terminal phosphanido ligand (63 and 62 Hz) were found to be smaller than those corresponding to the phosphane ligands (136 and 138 Hz). It can be attributed to a substantial reduction in the σ -orbital character of the Rh–PR₂ bond as compared to the Rh–phosphane,^[17a] and thus provides a useful tool for the identification of the terminal phosphanido ligand.

Complex **6** proved to be a fluxional species, since a single resonance ($^{31}\text{P}\{^1\text{H}\}$ NMR) and broad signals (^1H NMR) were observed at room temperature, but it gives sharp NMR signals at -70°C in $[\text{D}_8]\text{toluene}$. The most relevant resonances at this temperature were the hydride ligand ($\delta = -14.79$ ppm) and the PH proton ($\delta = 6.46$ ppm) showing a large $J(\text{H},\text{P}) = 391.0$ Hz coupling in the ^1H NMR spectrum.

This fluxionality can be ascribed to a prototropic shift of the PH proton from the phosphane to the phosphanido and, in good agreement, a low-barrier transition state of $+16.7$ kcal

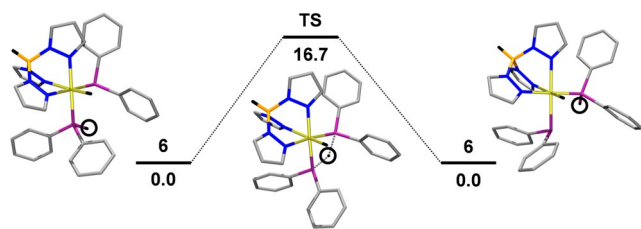


Figure 1. Energy profile (B3LYP-D3, 6–311G(d,p)/LanL2TZ(f)) for the shift of the PH proton from one phosphorus atom to the other in complex **6**. ΔG values in kcal mol⁻¹.

mol⁻¹ for this shift was calculated with DFT methods (Figure 1).

Complex **6** contains an intact diphenylphosphane ligand that could be appropriate for the study of the oxidative addition reaction of the P–H bond in the presence of a second rhodium center. A bimetallic system might work more efficiently for bond activation due to the cooperation of two metal centers.^[30] However, on mixing equimolar amounts of [Rh(Tp)(H)(PPh₂)(PPh₂)] (**6**) and [Rh(Tp)(C₂H₄)₂] (**1**) the immediate formation of [Rh(Tp)(C₂H₄)(PPh₂)] (**2**) was observed instead. Simultaneously, the bis(hydrido) dinuclear complex [(Tp)(H)Rh(μ-PPh₂)₂] (**3**) separated from the reaction media as an insoluble pale-yellow solid.

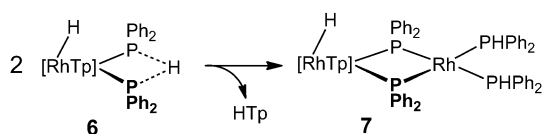
Complex **3** was characterized by analytical and spectroscopic data. Thus, the equivalent phosphanido bridges gave a triplet due to the coupling to the equivalent ¹⁰³Rh rhodium nuclei (*J*(P,Rh) = 92 Hz) in the ³¹P{¹H} NMR, whereas the hydride is observed as a doublet of triplets (²*J*(H,P) = 22.3, *J*(H,Rh) = 17.8 Hz) at $\delta = -12.54$ ppm in the ¹H NMR spectrum.

With this experiment in mind, it is easy to understand the strong influence of the experimental procedure on the preparation of complex [Rh(Tp)(C₂H₄)(PPh₂)] (**2**). Indeed, a fast addition of PPh₂ to [Rh(Tp)(C₂H₄)₂] (**1**) produces a high local concentration of the phosphane, suitable to render complex **6** and then the bis(hydride) dinuclear complex [(Tp)(H)Rh(μ-PPh₂)₂] (**3**) by reaction with unreacted complex **1**.

In addition, complex **6** in [D₆]benzene was slowly but quantitatively converted into the mixed-valence Rh^{III},Rh^I dinuclear complex [(Tp)(H)Rh^{III}(μ-PPh₂)₂Rh^I(PPh₂)₂] (**7**) (Scheme 3).

This reaction occurs with the concomitant extrusion of one Tp ligand as HTP (¹H NMR evidence). On a preparative scale, **7** was isolated as an orange microcrystalline solid in good yield after workup.

The molecular structure of **7**, displayed in Figure 2, shows two rhodium atoms bridged by two phosphanido ligands. The Rh^{III} atom, labelled as Rh1, completes a distorted octahedral geometry with the three N atoms of the Tp and the hydride



Scheme 3. Synthesis of complex **7**.

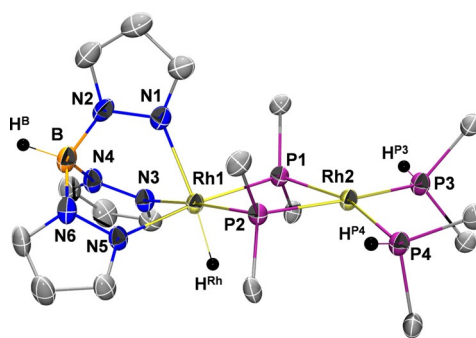


Figure 2. Molecular structure (ORTEP, ellipsoids set at 50% probability) of complex [(Tp)(H)Rh^{III}(μ-PPh₂)₂Rh^I(PPh₂)₂] (**7**). Selected bond lengths [Å] and angles [°]: Rh1–P1 2.291(1), Rh1–P2 2.274(1), Rh1–N1 2.173(3), Rh1–N3 2.150(3), Rh1–N5 2.133(3), Rh1–H^{Rh} 1.550(1), Rh2–P1 2.338(1), Rh2–P2 2.321(1), Rh2–P3 2.288(1), Rh2–P4 2.276(1), P1–Rh1–N5 172.8(8), P2–Rh1–N3 172.5(9), N1–Rh1–H^{Rh} 174.0(15), P1–Rh2–P4 162.7(4), P2–Rh2–P3 167.6(4). Only the C^{ipso} atoms of the phenyl groups are shown for clarity.

ligand, whereas the Rh^I center, labelled as Rh2, shows a square-planar environment with four P atoms (two from the phosphanido bridges and two from two diphenylphosphane ligands). The Rh1–P1 and Rh1–P2 bond distances are slightly shorter than the related Rh2–P1 and Rh2–P2, which is expected from the different oxidation states Rh1 (Rh^{III}) and Rh2 (Rh^I). The long Rh1,Rh2 distance of 3.6298(7) Å excludes any rhodium–rhodium interaction. On the whole, its molecular structure is quite similar to that of the related complex [(Tp)(H)Rh^{III}(μ-PPh₂)₂Rh^I(PPh₂)(PMe₃)], previously reported.^[29]

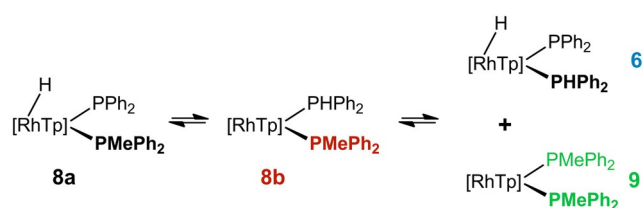
Spectroscopic data of **7** in [D₆]benzene agree with the structure found in the solid state. Thus, the ¹H NMR spectrum showed the hydride ligand at $\delta = -11.45$ ppm (td, ²*J*(H,P) = 22.4, *J*(H,Rh) = 18.3 Hz), whereas the equivalent PH protons produce a doublet of doublets at $\delta = 5.92$ ppm; the large coupling constant *J*(H,P) = 347.2 Hz agrees with both protons directly bonded to the respective phosphorus atoms. In addition, the ³¹P{¹H} showed two resonances at $\delta = 13.6$ (P^A) and -81.7 (P^B) ppm from a AA'MM'XY spin system (A, A' = PPh₂; M, M' = PPh₂, X, Y = ¹⁰³Rh). The high-field shift of the signal from the phosphanido ligands is in agreement with its bridging position between two rhodium atoms without a metal–metal bond.^[31]

Complex **7** is a rare example of a dinuclear bis(phosphanido) mixed-valence compound with a Rh^I,Rh^{III} core. Whereas there are several complexes of rhodium with two phosphanido bridges and the metal centers in the same oxidation state,^[32] there are limited examples of dirhodium mixed-valence bis(phosphanido) complexes. Nocera et al. described a series of Rh₂^{II,0}^[33] complexes with an octahedral Rh^{II} and trigonal bipyramidal Rh⁰ and Meek et al. reported dinuclear complexes with a square planar Rh center and a tetrahedral Rh center.^[34]

Reactions with PMePh₂ and PPh₃

Interestingly, the reaction of [Rh(Tp)(C₂H₄)(PPh₂)] (**2**) with the slightly less basic and more sterically demanding phosphane PMePh₂ resulted in an equilibrium distribution of the rhodium(III) species [Rh(Tp)(H)(PMePh₂)(PPh₂)] (**8a**) and the rhodi-

um(I) species $[\text{Rh}(\kappa^2\text{-Tp})(\text{PMePh}_2)(\text{PPhPh}_2)]$ (**8b**) in solution, which are formed in a 70:30 ratio at room temperature (Schemes 2 and 4). This ratio corresponds to a value of $K_{\text{eq}} = 2.33$ (**8b** \leftrightarrow **8a**) and $\Delta G_{298} = -0.50$ kcal mol⁻¹.



Scheme 4. Equilibrium between complexes **8a**, **8b**, **6**, and **9**.

In addition, small amounts of $[\text{Rh}(\text{Tp})(\text{H})(\text{PPhPh}_2)(\text{PPh}_2)]$ (**6**) and $[\text{Rh}(\kappa^2\text{-Tp})(\text{PMePh}_2)_2]$ (**9**) were also involved in the equilibrium (Scheme 4). They are the result of a phosphane exchange reaction undergone by the rhodium(I) complex **8b**.

Such equilibria were easily detected from the ¹H-¹H NOESY spectrum (Figure 3) because of the chemical exchange of the hydride ligand in **8a** and the PH proton of **8b** (left) as well as that of the methyl group of **8a**, **8b**, and **9** (right).

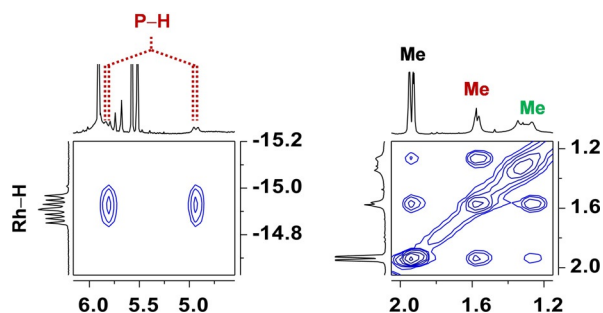


Figure 3. Two selected regions of the ¹H,¹H-noesy spectrum of **8** showing the negative cross-peaks due to the chemical exchange. Color code: $[\text{Rh}(\text{Tp})(\text{H})(\text{PMePh}_2)(\text{PPh}_2)]$ (**8a**, black), $[\text{Rh}(\kappa^2\text{-Tp})(\text{PMePh}_2)(\text{PPhPh}_2)]$ (**8b**, red) and $[\text{Rh}(\kappa^2\text{-Tp})(\text{PMePh}_2)_2]$ (**9**, green).

From these solutions a yellow solid (**8**) was isolated after workup in very good yield. The IR (ATR) spectrum shows bands at 2457 and 2082 cm⁻¹, assignable to the B–H and Rh–H stretching vibrations, respectively, so most probably complex **8** is the hydrido-phosphanido complex **8a** in the solid state.

A similar result occurred on addition of triphenylphosphane to $[\text{Rh}(\text{Tp})(\text{C}_2\text{H}_4)(\text{PPhPh}_2)]$ (**2**). Thus, monitoring the reaction by NMR spectroscopy, the complexes $[\text{Rh}(\text{Tp})(\text{H})(\text{PPh}_3)(\text{PPh}_2)]$ (**10a**), $[\text{Rh}(\kappa^2\text{-Tp})(\text{PPh}_3)(\text{PPhPh}_2)]$ (**10b**), $[\text{Rh}(\text{Tp})(\text{H})(\text{PPhPh}_2)(\text{PPh}_2)]$ (**6**) as well as $[\{(\text{Tp})(\text{H})\text{Rh}(\mu\text{-PPh}_2)\}_2]$ (**3**), $[\text{Rh}(\text{Tp})(\text{C}_2\text{H}_4)(\text{PPh}_3)]$ and free PPh_3 were identified in solution (see Supporting Information). In this case, complexes **10a/10b** were found to be formed in a 28:72 ratio at room temperature, which corresponds to a value of $K_{\text{eq}} = 0.39$ (**10b** \leftrightarrow **10a**) and $\Delta G_{298} = +0.56$ kcal mol⁻¹.

DFT calculations (B3LYP-D3, 6–311G(d,p)/LanL2TZ(f)) on the rhodium(I) complexes $[\text{Rh}(\kappa^2\text{-Tp})(\text{L})(\text{PPhPh}_2)]$ (L = PMe_2Ph **8b**,

PPh_3 **10b**) showed that they are square-planar species with the Tp ligand bonded to rhodium in a κ^2 -fashion and with the six-membered metallacycle $\text{Rh}(\text{NN})_2\text{B}$ showing a boat conformation (Figure 4).

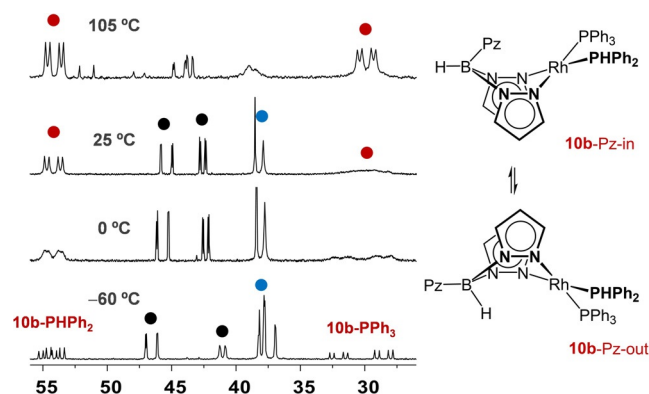


Figure 4. Selected region of the VT-³¹P{¹H} NMR spectra of the reaction $[\text{Rh}(\text{Tp})(\text{C}_2\text{H}_4)(\text{PPhPh}_2)]$ (**2**) with PPh_3 in $[\text{D}_8]$ toluene showing conformers **10b-Pz-in** and **10b-Pz-out**. Color code: $[\text{Rh}(\text{Tp})(\text{H})(\text{PPh}_3)(\text{PPh}_2)]$ (**10a**, black), $[\text{Rh}(\text{Tp})(\text{PPh}_3)(\text{PPhPh}_2)]$ (**10b**, red) and $[\text{Rh}(\text{Tp})(\text{H})(\text{PPhPh}_2)(\text{PPh}_2)]$ (**6**, blue).

This puckered structure leads to two conformers depending on the location of the uncoordinated pyrazolate ring, either inside or outside the pocket of the complex. Both conformers were clearly observed in the ³¹P{¹H} NMR spectra at –60 °C for **8b** and **10b**, and the equilibrium between them accounts for the intriguing spectra at room temperature, in which only one signal of the phosphorus atoms of **8b** and **10b** was clearly observed, whereas the second one is very broad and hard to distinguish from the baseline (Figure 4).

Comments on phosphane ligands promoting P–H bond activation reactions.

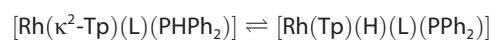
At first glance, one could argue that the oxidative addition reaction of the P–H bond in complexes $[\text{Rh}(\kappa^2\text{-Tp})(\text{L})(\text{PPhPh}_2)]$ would be favored by increasing the electron density at the rhodium center. As the electron richness of the metal in this series is given by the donor ability of the ligand L, this magnitude can be evaluated from the $\nu(\text{CO})$ stretching frequencies in complexes that only differ in the L ligand. For such purpose, the complexes $[\text{Rh}(\text{acac})(\text{CO})(\text{L})]$ (acac = acetylacetonate) that show a unique $\nu(\text{CO})$ band were chosen.^[35] The observed frequencies, collected in Table 1, give the following order of electron density: $\text{PMe}_3 > \text{PMe}_2\text{Ph} > \text{PMePh}_2 > \text{PPh}_3 > \text{PPhPh}_2$, which fit fairly well with the TEPs (Tolman electronic parameters) previously reported.^[36]

Table 1. IR $\nu(\text{CO})$ bands for the rhodium(I) complexes $[\text{Rh}(\text{acac})(\text{CO})(\text{L})]$ in toluene and computed cone angles. ^[37]					
	PMe_3	PMe_2Ph	PMePh_2	PPh_3	PPhPh_2
$\nu(\text{CO})$ [cm ⁻¹]	1968	1971	1975	1980	1982
cone angles [°]	118	122	136	145	128

From these data it is clear that electronic effects are not the most relevant factor to account for the above-described results. In particular, the richest (PMe_3) and poorest (PPhPh_2) rhodium centers give both the corresponding rhodium(III) hydrido-phosphanido complexes cleanly. In both cases, the reactions were found to be almost instantaneous, achieving completion in less than 5 min.

Interestingly, a nice fit is found if steric effects are considered instead. Indeed, the order according to the cone angle: $\text{PMe}_3 < \text{PMe}_2\text{Ph} < \text{PPhPh}_2 < \text{PMePh}_2 < \text{PPh}_3$ (Table 1) fit very well with the observed reactivity. Hydrido-phosphanido complexes were obtained for PMe_3 , PMe_2Ph and PPhPh_2 , whereas with the bigger ligands, PMePh_2 and PPh_3 , the equilibrium $[\text{Rh}(\kappa^2\text{-Tp})(\text{L})(\text{PPhPh}_2)] \rightleftharpoons [\text{Rh}(\text{Tp})(\text{H})(\text{L})(\text{PPh}_2)]$ was observed. In other words, it can be concluded that an increase in the size of the ligand diminishes the stability of the rhodium(III) oxidation state relative to the rhodium(I) counterpart, in such a way that an equilibrium between them is observed.

Since for complexes with the phosphanes PMePh_2 and PPh_3 both species are clearly observable by NMR, the thermodynamic parameters for the P–H oxidative addition reactions:



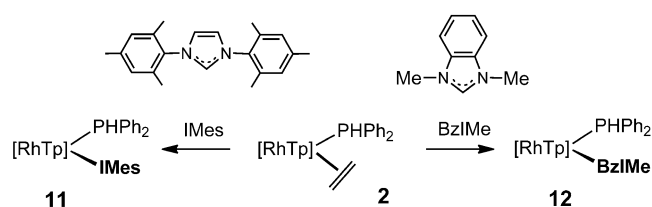
could be estimated from the Van 't Hoff plots (see Supporting Information). In both cases, a straight line was obtained giving values of $\Delta H = (-2.12 \pm 0.02)$ (**8**), (-2.64 ± 0.01) kcal mol⁻¹ (**10**) and $\Delta S = (-5.77 \pm 0.06)$ (**8**), (-10.74 ± 0.05) u.e. (**10**), which lead to ΔG at 298 K of -0.40 (**8**) and $+0.56$ kcal mol⁻¹ (**10**).

Although both reactions are exothermic, with similar values of enthalpy, the entropic contribution, more negative for the more steric demanding ligand (PPh_3), is the key factor that determines the lower stability of the rhodium(III) hydrido-phosphanido complex. Indeed, the change in the environment of rhodium from square-planar to octahedral, associated to the P–H bond activation reaction, produces more crowded complexes, which are more destabilized as the size of the ligand increases. Accordingly, complexes with the less demanding ligands PMe_3 , PMe_2Ph and PPhPh_2 are expected to be obtained as hydrido-phosphanido complexes as observed experimentally.

Reactions with N-heterocyclic carbenes

The ability of N-heterocyclic carbenes to promote P–H bond activation reactions was also tested by reacting $[\text{Rh}(\text{Tp})(\text{C}_2\text{H}_4)(\text{PPhPh}_2)]$ (**2**) with IMes (1,3-dimesitylimidazol-2-ylidene) and BzIme (1,3-dimethylbenzimidazol-2-ylidene). The products from the reactions were found to be the rhodium(I) complexes $[\text{Rh}(\kappa^2\text{-Tp})(\text{L})(\text{PPhPh}_2)]$ ($\text{L} = \text{IMes}$ **11**, BzIme **12**), which were isolated as yellow solids in good yields (Scheme 5).

Analytical and spectroscopic data of **11–12** agree with the proposed formulation. In particular, the PH proton was observed as a doublet of doublets at $\delta = 5.95$ (**11**) and 6.16 ppm (**12**) with large $J(\text{P,H}) = 332.5$ and 322.7 Hz and small ${}^2J(\text{H,Rh}) = 3.3$ and 1.1 Hz coupling constants, respectively, at low temperature. In addition, the abnormally large $J(\text{P,Rh})$ coupling con-



Scheme 5. Reactions of $[\text{Rh}(\text{Tp})(\text{C}_2\text{H}_4)(\text{PPhPh}_2)]$ (**2**) with IMes and BzIme.

stants of 195 and 192 Hz, respectively, would be related with a square-planar environment of rhodium, further confirmed by a X-ray diffraction study of complex **11**. Moreover, complex **11** was found to adopt the boat conformation in the solid state, with the uncoordinated pyrazolate ring dangling outside the pocket of the complex (**11-Pz-out**, Figure 5).

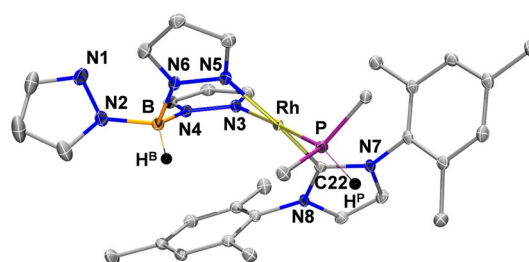


Figure 5. Molecular structure (ORTEP, ellipsoids set at 50% probability) of complex $[\text{Rh}(\kappa^2\text{-Tp})(\text{IMes})(\text{PPhPh}_2)]$ (**11-Pz-out**). Selected bond lengths [Å] and angles [°]: Rh–P 2.1985(5), Rh–N3 2.0957(14), Rh–N5 2.1014(14), Rh–C22 1.9903(16), P–Rh–N3 176.64(4), N5–Rh–C22 173.78(6).

DFT calculations (B3LYP-D3, 6–311G(d,p)/LanL2TZ(f)) on the conformer found in the solid state (**11-Pz-out**) as well as on that with the pyrazolate ring inside the pocket of the complex (**11-Pz-in**) revealed the former to be more stable than the latter by 3.9 kcal mol⁻¹. On the contrary, for complex **12** having the less demanding BzIme ligand, the conformer **12-Pz-in** was found to be more stable than **12-Pz-out** by 4.1 kcal mol⁻¹.

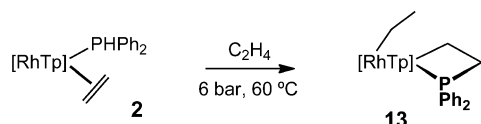
Complexes **11** and **12** were found to be fluxional species in solution. The analysis of the ¹H-¹H NOESY spectrum of **11** at room temperature revealed the presence of a dynamic process, in which the three pyrazolate rings, the four methyl groups at the *ortho* position of the IMes ligand, and the phenyl groups of the PPhPh_2 exchange. This process is slightly faster in the case of complex **12**, since at this temperature the ¹H NMR spectrum is close to that expected for the fast-exchange region. Such exchange could take place through the participation of pentacoordinated TBPY-5 species (the turnstile motion), as generally accepted for Tp-complexes.^[38] However, in the particular case of complex **11**, first a boat-to-boat inversion of the six-membered metallacycle $\text{Rh}(\text{NN})_2\text{B}$ is required to achieve the suitable conformer (**11-Pz-in**) to undergo $\kappa^2\text{-}\kappa^3$ isomerism.

The lack of a further P–H bond oxidative addition in the case of complexes **11** and **12** cannot be attributed to electronic effects as commented before. Indeed, they contain the more donating ligands (NHCs), with $\nu(\text{CO})$ stretching frequencies in

the complexes $[\text{Rh}(\text{acac})(\text{CO})(\text{L})]$ ($\text{L} = \text{IMes}, \text{BzIME}$) of 1955 and 1962 cm^{-1} , respectively. Most probably, the particular steric requirements of these ligands that place the steric demand in a specific direction account for their lack of further reactivity.

Reaction with ethylene

Heating a solution of $[\text{Rh}(\text{Tp})(\text{C}_2\text{H}_4)(\text{PPh}_2)]$ (**2**) in the presence of ethylene (6 bar) at 60°C for six days resulted in the novel rhodaphosphacyclobutane complex $[\text{Rh}(\text{Tp})(\eta^1\text{-Et})(\kappa^{\text{C-P}}\text{-CH}_2\text{CH}_2\text{PPh}_2)]$ (**13**, Scheme 6), which was isolated as an orange microcrystalline solid in good yields.



Scheme 6. Synthesis of the rhodaphosphacyclobutane complex **13** from **2**.

Control of the temperature and pressure of ethylene was crucial to get pure samples of **13** in such a way that complex **13** was contaminated with variable amounts of $[\{(\text{Tp})(\text{H})\text{Rh}(\mu\text{-PPh}_2)_2\}]$ (**3**) under lower pressures of ethylene and/or higher temperatures. As an example, this reaction was completed in 3 h at 105°C in $[\text{D}_8]$ toluene under an atmosphere of ethylene (2 bar), but the yield of **13** decreased up to 45%.

Complex **13** was identified as the rhodaphosphacyclobutane compound shown in Scheme 6 by its analytical and spectroscopic data. Thus, the ^1H NMR spectrum showed the diastereotopic CH_2 protons of ethyl group as two multiplets coupled to a triplet corresponding to the methyl group (Figure 6, in blue). In addition, the large coupling constant of the methylenic carbon to rhodium ($J(\text{C},\text{Rh}) = 24 \text{ Hz}$) clearly evidences the presence of a direct $\text{Rh}-\text{C}$ bond.^[39]

Signals due to the protons and carbons of the rhodaphosphacyclobutane moiety were clearly identified in the ^1H , $^{13}\text{C}\{^1\text{H}\}$, and $^{13}\text{C}\{^1\text{H},^{31}\text{P}\}$ NMR spectra (red and green, Figure 6). The methylenic protons and carbon directly attached to rhodium (H_2C^2 , in red) were upfield shifted relative to that bonded

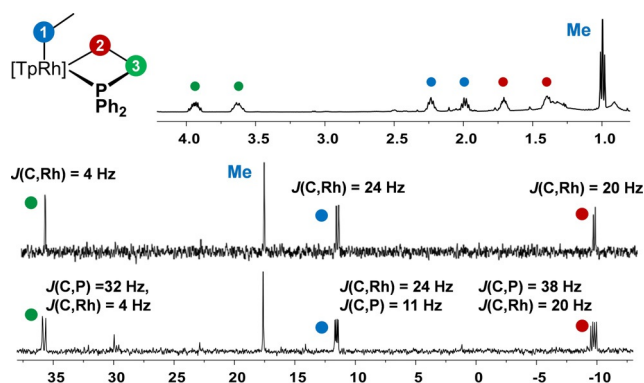


Figure 6. Selected regions of the ^1H (top), $^{13}\text{C}\{^1\text{H},^{31}\text{P}\}$ (middle), and $^{13}\text{C}\{^1\text{H}\}$ (bottom) NMR spectra of complex **13**.

directly to phosphorus (H_2C^3 , in green). In particular, the signal at $\delta = -9.5 \text{ ppm}$, with a large coupling constant to rhodium of 20 Hz, can be attributed to the CH_2 group directly attached to the rhodium atom (C^2), whereas that at $\delta = 36.0 \text{ ppm}$ ($^2J(\text{C},\text{Rh}) = 4 \text{ Hz}$) corresponds to C^3 directly bonded to phosphorus. A characteristic feature of the rhodaphosphetane moiety was present in the $^{31}\text{P}\{^1\text{H}\}$ NMR spectrum, which showed a doublet at $\delta = -36.1 \text{ ppm}$ ($J(\text{P},\text{Rh}) = 122 \text{ Hz}$) shifted upfield in about 70 ppm relative to **2** (48.1 ppm). Such a shift is diagnostic of a phosphorus atom in a four-membered metal-lacycle.^[40]

Repetitive attempts to grow single crystals of complex **13** under different conditions gave systematically very small and geminated microcrystals; thus, preventing further crystallographic structure determination. Hence, DFT geometry optimization was used to get structural information. An energy minimum was found for $[\text{Rh}(\text{Tp})(\eta^1\text{-Et})(\kappa^{\text{C-P}}\text{-CH}_2\text{CH}_2\text{PPh}_2)]$ (**13'**) (Figure 7), with rhodium in an almost octahedral environment.

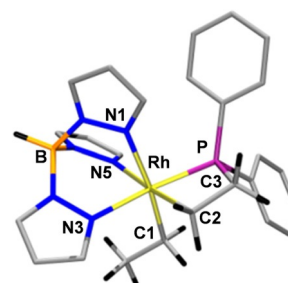


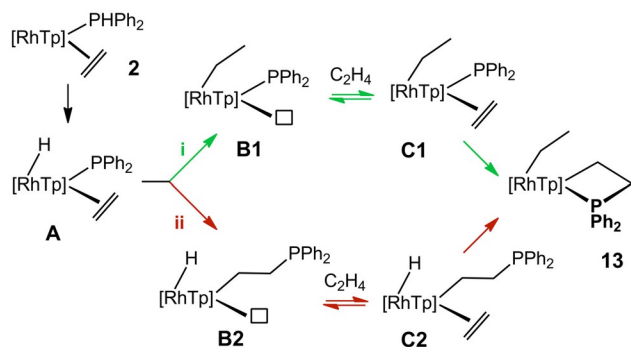
Figure 7. DFT-calculated structure (BP86, def2-TZVP, disp3) of complex $[\text{Rh}(\text{Tp})(\text{Et})(\kappa^{\text{C-P}}\text{-CH}_2\text{CH}_2\text{PPh}_2)]$ (**13'**).

The strong *trans* influence of the alkyl carbons ($\text{C}1$ and $\text{C}2$) is clearly demonstrated by the considerable elongation of the $\text{Rh}-\text{N}1$ and $\text{Rh}-\text{N}5$ bond distances (2.240 and 2.211 Å, respectively) in comparison with the other $\text{Rh}-\text{N}3$ bond (2.118 Å), which is *trans* to the phosphane. The four-membered ring slightly deviates from planarity ($\text{P}-\text{C}-\text{C}-\text{Rh}$ torsion angle of 12.55°). Among the endocyclic angles, the $\text{P}-\text{Rh}-\text{C}$ angle is the most acute (71.24°).

The formation of the rhodaphosphacyclobutane **13** is remarkable as there are very few examples of metallaphosphacyclobutanes, mainly limited to ruthenium^[41] and palladium^[42] complexes. Rhodium phosphacyclobutanes are also known, however they have mainly been obtained from *ortho* metalation of phosphanes.^[43] To our knowledge, this is the first example of a rhodaphosphacyclobutane derived from an alkene, as well as the first example of insertion of a non-activated olefin (ethylene) into a $\text{Rh}-\text{P}$ bond. Moreover, reactions leading to $\text{P}-\text{C}$ bond formation with non-activated olefins such as ethylene are essentially absent in the literature.^[1b,d,f] Notable examples include a nickel phosphanidene complex that can undergo ethylene insertion leading to an organic phosphirane via an intermediate four-membered nickel phosphacycle,^[44] the nickel-mediated reaction of a primary phosphane to a functionalized phosphane through ethylene insertion,^[19] and a ruthenium

phosphide species which reacts with olefins, including ethylene and 1-hexene, to yield metallaphosphacyclobutanes.^[41]

The most plausible mechanistic pathways to **13** are shown in Scheme 7 and involve two inner-sphere ethylene insertions into the Rh–H and the Rh–P bonds. In both cases, the first step is the oxidative addition of diphenylphosphane to give intermediate **A**. In the next step, insertion of the coordinated ethylene can occur into either the Rh–H (Scheme 7, in green) or the Rh–P bond (Scheme 7, in red). Coordination of ethylene on the resulting intermediates (**B1/B2**) would produce **C1/C2**, suitable for the second ethylene insertion into the Rh–P/Rh–H bonds, respectively.



Scheme 7. Plausible mechanistic pathways for the formation of complex **13** from **2**. Path (i) starts with ethylene insertion into the Rh–H bond, whereas path (ii) starts with ethylene insertion into the Rh–P bond.

The first step in both pathways is the oxidative addition of the P–H bond of complex **2** to form intermediate **A**. This reaction has a relative high barrier of +28.7 kcal mol^{−1} according to DFT calculations (Figure 8). This seems to be the rate-determining step for the formation of **13**. Experimentally the reaction requires heating to 60 °C for six days to reach completion, from which one can estimate an activation barrier of about +27.3 kcal mol^{−1} using the Eyring equation,^[45] which is in reasonable agreement with the slightly overestimated DFT barrier.

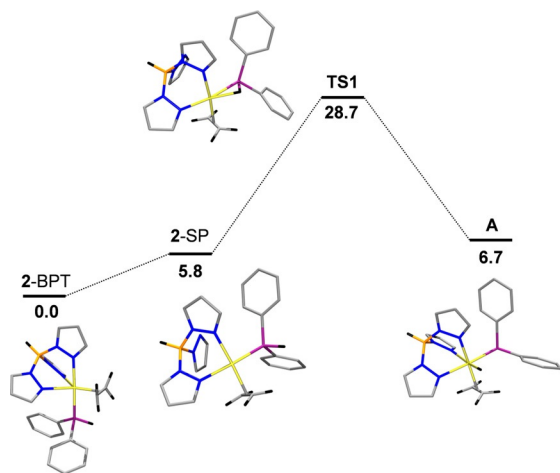


Figure 8. DFT-computed (BP86, def2-TZVP, disp3) barrier for oxidative addition of the P–H bond in complex **2** to form intermediate **A**.

The two most logical pathways for the formation of complex **13** from **A** were both computed with DFT calculations. The green pathway through intermediates **B1** and **C1** is clearly the preferred pathway, and has low-barrier and very accessible transition states once **A** is formed (Figure 9). The alternative red pathway via intermediates **B2** and **C2** has much higher barriers (Figure 10), and the formation of intermediate **B2'** from **B2** involving dissociation of the Rh–P bond of the rhodaphosphacyclobutane ring (+31.3 kcal mol^{−1}) is even more endergonic than **TS1** (Figure 8).

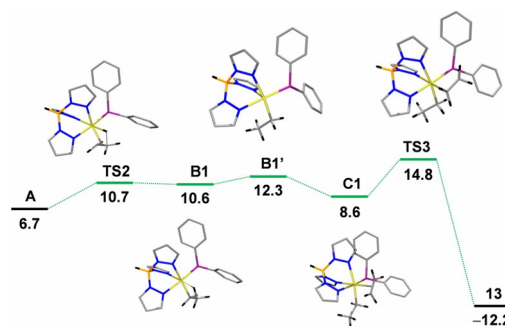


Figure 9. Green pathway: DFT-computed (BP86, def2-TZVP, disp3) pathway for the formation of complex **13** from intermediate **A** through **B1** and **C1**.

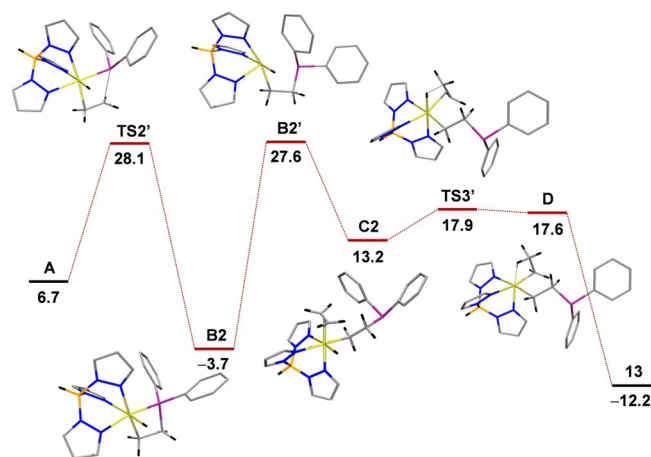


Figure 10. Red pathway: DFT-computed (BP86, def2-TZVP, disp3) pathway for the formation of complex **13** from intermediate **A** through **B2** and **C2**.

It is therefore clear that the reaction to form complex **13** should follow the green pathway (through intermediates **B1** and **C1**) as shown in Figure 9. The mechanism described herein is distinct from the ruthenium chemistry described by Rosenberg et al., in which the ruthenium species undergoes a 2+2 cycloaddition through a Ru phosphanidene (Ru=P) intermediate,^[41] whereas the chemistry reported here occurs through the rhodium hydrido-phosphanido intermediate **A**.

Our results indicate a preference for ethylene insertion into the Rh–H bond and are in agreement with related DFT studies^[46] on alkyne insertion into metal-phosphanide bonds for which calculations showed that alkyne insertion into a M–H bond should be much easier compared to a M–P bond (M = Pd, Ni, Pt, and Rh).

Attempts to eliminate ethane and PEtPPh_2 from **13** aimed to close a hypothetical dual hydrophosphanation/hydrogenation catalytic cycle were tested using HPPH_2 as proton source. Therefore, complex **13** was heated in the presence of PPhPh_2 (20 mol equiv) at 80°C under an atmosphere of ethylene (6 bar). PEtPPh_2 (20%) and ethane were observed as products, but the major component of the reaction mixture was found to be $\text{Ph}_2\text{P}-\text{PPh}_2$ (80%), the product from the dehydrocoupling reaction. Even after prolonged heating of **13** (105°C for a week) no evidence for ethylene deinsertion was observed. Other ligands were also added to **13** to favor reductive elimination. However, no reaction was observed with CO (1 atm., 80°C , 48 h) by ^1H and ^{31}P NMR spectroscopy.

Reactions with OPHPh_2

Diphenylphosphane oxide reacts with $[\text{Rh}(\text{Tp})(\text{C}_2\text{H}_4)(\text{PPhPh}_2)]$ (**2**) to give $[\text{Rh}(\text{Tp})(\text{H})(\text{P}(\text{O})\text{Ph}_2)(\text{PPhPh}_2)]$ (**14**), which was fully characterized by analytical and spectroscopic methods, including a X-ray crystallographic study (Figure 11).

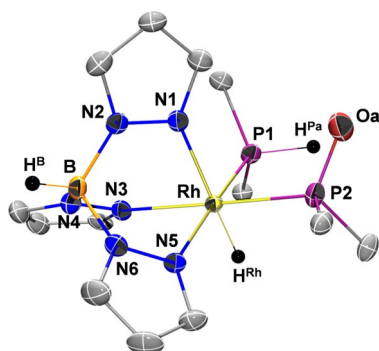


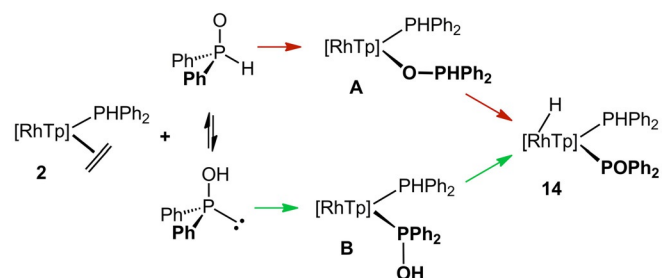
Figure 11. Molecular structure (ORTEP, ellipsoids set at 50% probability) of complex $[\text{Rh}(\text{Tp})(\text{H})(\text{P}(\text{O})\text{Ph}_2)(\text{PPhPh}_2)]$ (**14**). Selected bond lengths [Å] and angles [$^\circ$]: Rh–P1 2.238(2), Rh–P2 2.268(2), Rh–N1 2.162(4), Rh–N3 2.164(4), Rh–N5 2.122(4), P2–Oa 1.511(6), P1–Rh–N5 174.5(2), P2–Rh–N3 179.0(2), N1–Rh–H^{Rh} 176(3). Only the C^{ipso} of the phenyl rings are shown for clarity.

Its molecular structure shows the rhodium atom in the center of a slightly distorted octahedron bound to the three nitrogen atoms of the Tp ligand, two phosphorus atoms coming from the phosphanido and the phosphane oxide, respectively, and the hydride ligand. The remaining proton is bound to a phosphorus atom, as deduced by its signal at $\delta = 7.17$ ppm ($J(\text{H},\text{P}) = 410.2$, $^2J(\text{H},\text{P}) = 10.5$ Hz) in the ^1H NMR spectrum, but it could not be located in the structure due to the disorder of the oxygen atom over the two phosphorus atoms (75.3(14) and 24.7(14)% relative abundance).

Spectroscopic data of **14** in solution agreed with the structure shown in Figure 11. Thus, the $^{31}\text{P}\{^1\text{H}\}$ NMR spectrum showed two doublets of doublets at $\delta = 75.7$ and 33.5 ppm; the peak at high field has been assigned to the phosphane PPhPh_2 ligand. The hydride ligand resonates at $\delta = -13.74$ as a doublet of doublets of doublets by coupling to the two *cis* P atoms ($^2J(\text{H},\text{P}) = 23.2$ and 20.4 Hz) and to the ^{103}Rh nuclei ($^1J(\text{H},\text{Rh}) = 16.0$ Hz), whereas the PH proton was observed at

$\delta = 7.17$ ppm in the ^1H NMR spectrum. Moreover, $^1\text{H}-^{31}\text{P}$ HMBC NMR experiments (with $J(\text{H},\text{P}) = 10$ and 400 Hz) showed that this proton was strongly coupled to the phosphane ligand ($J(\text{H},\text{P}) = 410.1$) and in less extension to the POPPh_2 ligand ($J(\text{H},\text{P}) = 10.5$ Hz). These observations along with its molecular structure (Figure 11, in which both phosphorus atoms are coordinated to rhodium) definitively confirm that the hydride ligand comes from the phosphane oxide (OPHPh_2) instead of the phosphane PPhPh_2 .

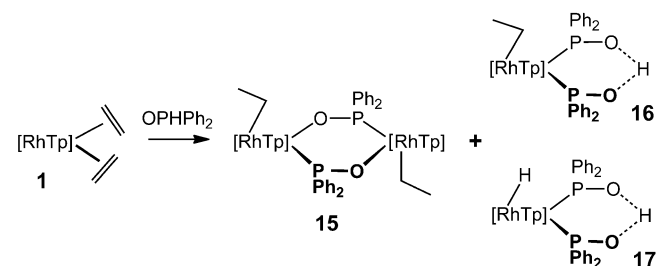
A plausible sequence of reactions in the synthesis of **14** is shown in Scheme 8. The red pathway starts with the coordina-



Scheme 8. Plausible sequence of reactions for the synthesis of **14** from **2** and OPHPh_2 .

tion of diposphane oxide to render intermediate **A**, followed by the activation of P–H bond. This step requires decoordination of one of the pyrazolate arms to allow the approaching of the P–H bond to rhodium. The participation of the tautomer hydroxydiphenylphosphane would give intermediate **B** followed by an easy O–H bond activation reaction (green pathway). Although both possibilities could be operative, we believe that the pathway marked in green is more plausible, in spite of the smaller abundance of the hydroxy tautomer in the equilibrium,^[47] because of the type of bonds involved. Indeed, such activations through the tautomer phosphinous acid have been previously proposed for ruthenium complexes on the basis of DFT calculations.^[12]

Interestingly, the reaction of OPHPh_2 with the bis(ethylene) complex $[\text{Rh}(\text{Tp})(\text{C}_2\text{H}_4)_2]$ (**1**) (in 1:1 molar ratio) did not give the mononuclear complex $[\text{Rh}(\text{Tp})(\text{C}_2\text{H}_4)(\text{OPHPh}_2)]$ (analogous to **2**), but the bis(η^1 -ethyl) dinuclear complex $[\{(\text{Tp})(\eta^1\text{-Et})\text{Rh}(\mu\text{-OPPh}_2)\}_2]$ (**15**) along with the mononuclear complexes $[\text{Rh}(\text{Tp})(\eta^1\text{-R})(\text{POPPh}_2)(\text{POHPh}_2)]$ (R = Et, **16** and H, **17**) (Scheme 9). From these solutions, complex **15** was isolated



Scheme 9. Reaction of **1** with OPHPh_2 .

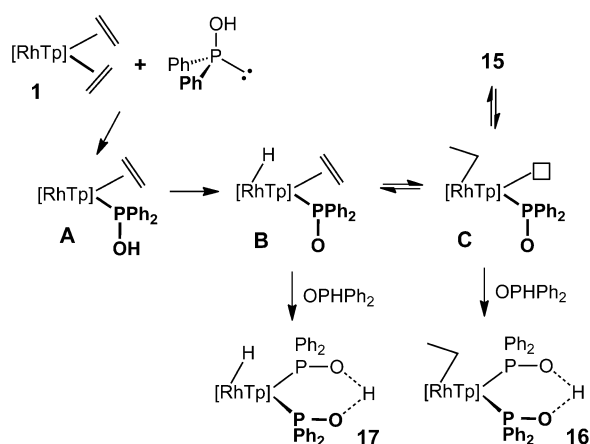
after work-up, whereas a mixture of complexes **16** and **17** was isolated in high yield if solutions of **15** in the presence of two molar equivalents of OPhPh₂ were heated for 14 h at 60 °C in toluene.

The dinuclear nature of **15** is evident from the ³¹P{¹H} NMR, which shows a multiplet corresponding to the AA' part of an AA'XX' spin system (A, A' = ³¹P; X, X' = ¹⁰³Rh) for the two equivalent phosphorus nuclei. The ethyl group was clearly observed as three signals (1:1:3 ratio) in the ¹H NMR spectrum with the methylenic protons strongly coupled to the phosphorus atom according to the ¹H-³¹P HMBC spectrum.

Complexes **16** and **17** could not be separated because of their high tendency to crystallize together in a disordered manner. Indeed, all single crystals studied by X-ray methods revealed that they contained both complexes in an approximate 1:1 ratio.^[48] Nonetheless, spectroscopic data of the isolated solid agrees with a mixture of **16** and **17** in a 2:1 molar ratio. Thus, a broad signal, corresponding to the hydrogen interacting with the two oxygens, was found at δ = 18.34 ppm in the ¹H NMR spectrum. The methylenic protons of the ethyl ligand in **16** were observed at δ = 2.22 ppm as a quartet of triplets of doublets because of the coupling with the three protons of the adjacent methyl group (³J(H,H) = 7.5 Hz), the two equivalent phosphorus atoms (³J(H,P) = 4.1 Hz) and ¹⁰³Rh (²J(H,Rh) = 1.9 Hz). The hydride ligand in **17** was detected at δ = -12.99 ppm as a triplet of doublets because of the coupling with the two equivalent phosphorus atoms (²J(H,P) = 21.7 Hz) and ¹⁰³Rh (J(H,Rh) = 16.7 Hz).

Scheme 10 shows a plausible sequence of reactions that accounts for the synthesis of **15–17** from the reactions of [Rh(Tp)(C₂H₄)₂] (**1**) with OPhPh₂. The first part of the reaction would consist in the coordination of the hydroxydiphenyl tautomer to give intermediate **A**, followed by the oxidative addition reaction of the O–H bond to give species **B**, as previously commented for complex **14**.

From **B**, ethylene replacement by a new molecule of OPhPh₂ would give the hydride complex [Rh(Tp)(H)(POPh₂)(POHPh₂)] (**17**), but a competitive insertion reaction of the hydride ligand into the Rh–ethylene bond would lead to intermediate **C**. From **C**, a dimerization would render the dinuclear complex



Scheme 10. Plausible sequence of reactions to complexes **15–17**.

[[Tp](η¹-Et)Rh(μ-OPPh₂)₂] (**15**), whereas coordination of OPhPh₂ would produce the mononuclear complex [Rh(Tp)(η¹-Et)(POPh₂)(POHPh₂)] (**16**).

The proposed equilibrium between complex **15** and intermediates **B** and **C** has been verified by the reaction of **15** with OPhPh₂ (in 1:2 molar ratio), which systematically gives a mixture of the mononuclear complexes **16** and **17** in a 2:1 ratio. Since no change of this ratio was observed on heating this mixture for prolonged time, complexes **16** and **17** are not in equilibrium and, most probably, they arise from intermediates **B** and **C**, respectively. This ratio could represent the relative rates for OPhPh₂ coordination to **B/C** (assuming a fast equilibrium **B** ⇌ **C**), or alternatively the ratio of **B** and **C** in the equilibrium if coordination of OPhPh₂ were faster. However, considering the low ΔG values for hydride insertions into Rh–ethylene bonds,^[49] the first possibility seems to be more plausible.

Conclusions

The combination of tridentate hydridotris(pyrazolyl)borate and phosphane ligands on rhodium provides an useful platform for the selective oxidative addition reaction of the P–H bond in diphenylphosphane to give the new hydrido-phosphanido complexes [Rh(Tp)(H)(L)(PPh₂)] (L = PMe₃, PMe₃Ph, PPh₂). Increasing the steric bulk of the phosphane by using PMePh₂ or PPh₃ also results in the corresponding hydrido-phosphanido complexes, but in these cases they establish an equilibrium with the corresponding square-planar rhodium(I) complexes with a κ²-coordinated Tp ligand. The thermodynamic parameters for such equilibria: [Rh(κ²-Tp)(L)(PPh₂)] ⇌ [Rh(Tp)(H)(L)(PPh₂)] (L = PMePh₂, PPh₃), obtained from the Van 't Hoff plots, indicate both reactions to be slightly exothermic (ΔH = (−2.12 ± 0.02) and (−2.64 ± 0.01) kcal mol^{−1}) with a negative entropic contribution; larger for the bulkier PPh₃ than for PMePh₂ (ΔS = (−10.74 ± 0.05) and (−5.77 ± 0.06) u.e., respectively). These results strongly support that steric factors, over electronic effects, govern the formation of the final products. Indeed, both the richest (with PMe₃) and poorest (with PPh₂) rhodium centers give the corresponding rhodium(III) hydrido-phosphanido complexes cleanly. However, complexes with the highly donating NHCs ligands IMes and BzIME remained in the rhodium(I) oxidation state under similar conditions. In this case, the lack of reactivity can be attributed to the particular steric requirements of these ligands that direct the steric demands in a specific direction, hindering access to the P–H bond activation transition state.

The reaction of [Rh(Tp)(C₂H₄)(PPh₂)] with ethylene leads to the unique rhodaphosphacyclobutane complex [Rh(Tp)(η¹-Et)(κ^{C-P}-CH₂CH₂PPh₂)]. It is the result of a double ethylene insertion into the Rh–H and Rh–P bonds. Computational studies provided insights into the reaction mechanism, revealing that the lowest energy pathway involves oxidative addition of the P–H bond in **2** to form intermediate **A**, followed by low-barrier reaction steps involving ethylene insertion into the formed Rh–H and Rh–P bonds.

A formal P–H bond activation of phosphane oxide also takes place to give the related hydrido complex

[RhTp(H)(PPh₂)(POPh₂)], in the reaction of [Rh(Tp)(C₂H₄)(PPh₂)] with OPPh₂, but ethyl complexes result from hydride insertion into Rh–ethylene bond in the reaction with [Rh(Tp)(C₂H₄)₂]. In these reactions, the participation of the phosphinous acid tautomer is proposed, firstly coordinating to the metal through the phosphorous atom, and then transferring the O–H proton to the rhodium.

We believe that the results reported here expand the knowledge on oxidative addition reactions of secondary phosphanes to rhodium, which can be useful for the design of catalyzed processes leading to green syntheses of phosphanes.

Experimental Section

All the operations were carried out under an argon atmosphere using standard Schlenk techniques as well as dry-box facilities. The complexes [Rh(Tp)(C₂H₄)₂] (1),^[38,50] [Rh(Tp)(C₂H₄)(PPh₂)] (2),^[29] and [Rh(Tp)(H)(PMe₂)(PPh₂)] (4)^[29] were prepared according to literature methods. Diphenylphosphane purchased from Aldrich was found to contain about 4% of diphenylphosphane oxide. The oxide was removed by silica gel column chromatography using diethyl ether as eluent. Diethyl ether was then evaporated under vacuum. Elemental analyses (carbon, hydrogen, and nitrogen) were carried out with a PerkinElmer 2400 CHNS/O microanalyzer. Mass spectra and high-resolution mass spectra of complexes were acquired on a Bruker Esquire3000 plus (ESI+) and a Bruker MicroTOF-Q (ESI+) spectrometers, respectively. NMR spectra were recorded on Bruker AV300, AV400 and AV500 spectrometers operating at 300.13, 400.13 and 500.13 MHz, respectively, for ¹H. Chemical shifts are reported in ppm and referenced to SiMe₄, using the internal signal of the deuterated solvent (¹H and ¹³C) and external H₃PO₄ 85% in water (³¹P) and HBF₄·OEt₂ 15% in [D₆]benzene (¹¹B). IR spectra of solid samples were recorded with a PerkinElmer 100 FT-IR spectrometer (4000–400 cm⁻¹) equipped with attenuated total reflectance (ATR). For the labeling of protons and carbons see the Supporting Information.

Synthesis of the complexes

[[Rh(Tp)(H)Rh(μ-PPh₂)₂]] (3): An NMR tube was charged with [Rh(Tp)(C₂H₄)₂] (1, 9.0 mg, 0.024 mmol) and [Rh(Tp)(H)(PPh₂)(PPh₂)] (6, 16.6 mg, 0.024 mmol) and then [D₆]benzene (0.5 mL) was added. The reaction was monitored by ¹H and ³¹P{¹H} NMR showing the immediate formation of [Rh(Tp)(C₂H₄)(PPh₂)] (2) while a white solid corresponding to complex 3 precipitated. The resulting suspension was centrifuged, decanted and the remaining solid was washed with hexane (3×0.5 mL) and dried under vacuum. Yield: 7.5 mg (63%). IR(ATR): ν(B–H) 2485 cm⁻¹ (m), ν(Rh–H) 2064 cm⁻¹ (m); ¹H NMR (400.13 MHz, [D₆]benzene, 25 °C): δ = 9.91 (brs, 2H, PPh^{o1}), 7.68 (d, ³J(H,H) = 2.3 Hz, 2H, Pz^{B5}), 7.52 (brs, 2H, PPh^{m1}), 7.38 (dd, ³J(H,H) = 2.4, ⁵J(H,H) = 0.7 Hz, 4H, Pz^{A5}), 7.17 (dd, ³J(H,H) = 2.4 Hz, 2H, Pz^{B3}), 7.07 (t, ³J(H,H) = 6.8 Hz, 2H, PPh^{o2}), 7.01 (m, 4H, PPh^{o2}), 6.81 (t, ³J(H,H) = 7.5 Hz, 2H, PPh^{m2}), 6.76 (brs, 2H, PPh^{m1}), 6.65 (dd, ³J(H,H) = 2.0, ⁴J(H,H) = 0.7 Hz, 4H, Pz^{A3}), 6.64 (brs, 2H, PPh^{o1}), 6.60 (t, ³J(H,H) = 7.7 Hz, 4H, PPh^{m2}), 5.78 (t, ³J(H,H) = 2.1 Hz, 2H, Pz^{B4}), 5.67 (t, ³J(H,H) = 2.2 Hz, 4H, Pz^{A4}), –12.54 ppm (td, ²J(H,P) = 22.3, J(H,Rh) = 17.8 Hz, 1H, Rh–H); ³¹P{¹H} NMR ([D₆]benzene, 25 °C): δ = –48.9 ppm (t, J(P,Rh) = 92 Hz); ¹¹B{¹H} NMR (128.4 MHz, [D₆]benzene, 25 °C): δ = –3.83 ppm (s, BH); elemental analysis calcd (%) for C₄₂H₄₂N₂B₂P₂Rh₂ (1004.24): C 50.23, H 4.22, N 16.74; found: C 49.80, H 4.35, N 17.02.

[Rh(Tp)(H)(PMe₂Ph)(PPh₂)] (5): Dimethylphenylphosphane (25 μL, 0.18 mmol) was added to a yellow solution of [Rh(Tp)(C₂H₄)(PPh₂)] (2, 94.5 mg, 0.18 mmol) in toluene (4 mL) producing an immediate color change from yellow to orange. After stirring for 10 min, the solution was concentrated to 0.5 mL and precipitated with hexane (6 mL). The orange solid that precipitated was separated by decantation, washed with cold hexane (1×2 mL) and dried under vacuum. Yield: 83.4 mg (73%). IR(ATR): ν(B–H) 2460 cm⁻¹ (m), ν(Rh–H) 2142 cm⁻¹ (m); ¹H NMR (500.13 MHz, [D₈]toluene, 25 °C): δ = 8.16 (t, ³J(H,H) = ³J(H,P) = 6.2 Hz, 2H, PPh^{o1}), 7.57 (d, ³J(H,H) = 2.1 Hz, 1H, Pz^{B5}), 7.46 (d, ³J(H,H) = 1.2 Hz, 1H, Pz^{B3}), 7.33 (d, ³J(H,H) = 2.1 Hz, 1H, Pz^{A5}), 7.26 (brt, ³J(H,H) = ³J(H,P) = 2.1 Hz, 1H, Pz^{C5}), 7.23 (m, 4H, PMe₂Ph^o + PPh^{m1}), 7.12 (t, ³J(H,H) = 7.2 Hz, 1H, PPh^{o1}), 7.10 (brs, 1H, Pz^{C3}), 6.96 (t, ³J(H,H) = 7.3 Hz, 1H, PMe₂Ph^o), 6.92 (t, ³J(H,H) = 7.3 Hz, 2H, PMe₂Ph^m), 6.83 (t, ³J(H,H) = ³J(H,P) = 7.2 Hz, 2H, PPh^{o2}), 6.81 (hidden, 1H, PPh^{o2}), 6.73 (t, ³J(H,H) = 7.3, 2H, PPh^{m2}), 6.66 (d, ³J(H,H) = 2.1 Hz, 1H, Pz^{A3}), 5.96 (t, ³J(H,H) = 2.0 Hz, 1H, Pz^{B4}), 5.61 (t, ³J(H,H) = 2.1 Hz, 1H, Pz^{A4}), 5.53 (m, 1H, Pz^{C4}), 4.57 (brd, J(H,B) = 135.1 Hz, 1H, HB), 1.64 (d, J(H,P) = 9.6 Hz, 3H, PMe), 1.45 (d, J(H,P) = 9.6 Hz, 3H, PMe), –15.44 ppm (ddd, ²J(H,P) = 27.1, 9.6 Hz, J(H,Rh) = 16.0 Hz, Rh–H); ³¹P{¹H} NMR (202.5 MHz, [D₈]toluene, 25 °C): δ = 35.4 (dd, J(P,Rh) = 62 Hz, ²J(P,P) = 16 Hz, 1P, PPh₂), 14.5 ppm (dd, J(P,Rh) = 138 Hz, ²J(P,P) = 16 Hz, 1P, PMe₂Ph); ¹¹B{¹H} NMR (160.5 MHz, [D₈]toluene, 25 °C): δ = –3.44 ppm (s, BH); HRMS *m/z* calcd for C₂₉H₃₃BN₆P₂Rh [M+H]⁺ 641.1390, found: 641.1397 (error (mD) = –0.7); elemental analysis calcd (%) for C₂₉H₃₂N₆BP₂Rh (640.27): C 54.40, H 5.04, N 13.13; found: C 54.12, H 4.87, N 12.99.

[Rh(Tp)(H)(PPh₂)(PPh₂)] (6): Diphenylphosphane (26 μL, 0.15 mmol) was added to a yellow solution of [Rh(Tp)(C₂H₄)₂] (1, 78.8 mg, 0.15 mmol) in toluene (4 mL). An immediate color change to bright orange was observed. After stirring for 10 min, the solution was concentrated to 0.5 mL and hexane (5 mL) was added. The yellow solid that precipitated was separated by decantation and washed with hexane. Yield: 82 mg (81%). IR(ATR): ν(B–H) 2462 cm⁻¹ (m), ν(P–H) 2310 cm⁻¹ (m), ν(Rh–H) 2117 cm⁻¹ (m); ¹H NMR (400.13 MHz, [D₈]toluene, –70 °C): δ = 8.19 (s, 1H, Pz^{C3}), 8.08 (brs, 2H, PPh^{o1}), 7.75 (brs, 2H, PPh^{o2}), 7.61 (brt, ³J(H,H) = ³J(H,P) = 7.4 Hz, 2H, HPPH^{o1}), 7.46 (s, 1H, Pz^{B5}), 7.37 (s, 2H, Pz^{A5} + C⁵), 7.16 (s, 2H, PPh^{m1}), 6.97 (m, 7H, PPh^{(m+p)2} + HPPH^{(m+p)1} + PPh^{p1}), 6.89 (s, 1H, Pz^{A3}), 6.76 (t, ³J(H,H) = 6.6 Hz, 1H, HPPH^{p2}), 6.63 (t, ³J(H,H) = 6.6 Hz, 2H, HPPH^{m2}), 6.53 (t, ³J(H,H) = ³J(H,P) = 6.9 Hz, 2H, HPPH^{o2}), 6.46 (dd, ¹J(H,P) = 391.0 Hz, ³J(H,Rh) = 10.0 Hz, 1H, PPh₂), 5.85 (brs, 1H, Pz^{C4}), 5.83 (brs, 1H, Pz^{B3}), 5.63 (brs, 1H, Pz^{B4}), 5.55 (brs, 1H, Pz^{A4}) –14.79 ppm (dt, ²J(H,P) = 26.8, ²J(H,P) = J(H,Rh) = 13.0 Hz, 1H, Rh–H); ³¹P{¹H} NMR (162.0 MHz, [D₈]toluene, –70 °C): δ = 37.9 (brd, J(P,Rh) = 70 Hz, 1P, PPh₂), 37.1 ppm (brd, J(P,Rh) = 143 Hz, 1P, HPPH₂); ¹¹B{¹H} NMR (128.4 MHz, [D₈]toluene, –70 °C): δ = –3.77 ppm (s, BH); HRMS *m/z* calcd for C₃₃H₃₃BN₆P₂Rh [M+H]⁺ 689.1390, found: 689.1368 (error (mD) = 2.2); elemental analysis calcd (%) for C₃₃H₃₂N₆BP₂Rh (687.30): C 57.58, H 4.69, N 12.21; found: C 56.95, H 5.05, N 12.64.

[(Tp)(H)Rh^{III}(μ-PPh₂)₂Rh^I(PPh₂)₂] (7): Diphenylphosphane (19.7 μL, 0.114 mmol) was added to a solution of [Rh(Tp)(C₂H₄)(PPh₂)] (2, 60.5 mg, 0.114 mmol) in toluene (5 mL). After stirring for 3 days, the solution was concentrated to 0.5 mL, layered with hexane (6 mL) and left undisturbed overnight. The orange microcrystals that precipitated were separated by decantation, washed with cold hexane (1×2 mL) and dried under vacuum. Yield: 49.1 mg (74%). IR(ATR): ν(B–H) 2477 cm⁻¹ (m), ν(Rh–H) 2064 cm⁻¹ (m); ¹H RMN (300.13 MHz, [D₆]benzene, 25 °C): δ 8.38 (t, ³J(H,H) = ³J(H,P) = 7.2, 4H, PPh^{o1}), 8.03 (t, ³J(H,H) = 7.2 Hz, 4H, PPh^{o2}), 7.37 (d, ³J(H,H) = 2.1 Hz, 1H, Pz^{B5}), 7.35 (m, 4H, HPPH^{o1}), 7.34 (dd,

$^3J(\text{H,H}) = 2.3$ Hz, 2H, Pz^{A5}), 7.07 (d, $^3J(\text{H,H}) = 1.8$ Hz, 2H, Pz^{A3}), 7.03 (t, $^3J(\text{H,H}) = 7.6$ Hz, 4H, PPh^{m2}), 6.94 (m, 16H, $\text{HPPH}^{\text{o2}} + \text{PPh}^{\text{m1}} + \text{PPh}^{\text{o2}} + \text{HPPH}^{\text{(m+p1)}}$), 6.84 (m, 8H, $\text{HPPH}^{\text{(m+p2)}} + \text{PPh}^{\text{p1}}$), 6.14 (d, $^3J(\text{H,H}) = 1.9$ Hz, 1H, Pz^{B3}), 5.92 (dd, $J(\text{H,P}) = 347.2$ Hz, $^2J(\text{H,Rh}) = 11.3$ Hz, 1H, HP), 5.70 (t, $^3J(\text{H,H}) = 2.1$ Hz, 2H, Pz^{A4}), 5.47 (t, $^3J(\text{H,H}) = 2.1$ Hz, 1H, Pz^{B4}), 4.55 (brd, $^1J(\text{H,B}) = 130.9$ Hz, 1H, HB), -11.45 ppm (td, $^2J(\text{H,P}) = 22.4$, $J(\text{H,Rh}) = 18.3$ Hz, 1H, Rh–H); $^{31}\text{P}\{^1\text{H}\}$ RMN (121.5 MHz, $[\text{D}_6]\text{benzene}$, 25 °C): spin system AA'MM'XY (A, A' = PPhPh_2 , M, M' = PPh_2 , X, Y = ^{103}Rh); $\delta(\text{P}^{\text{A}}) = 13.6$ ppm, $\delta(\text{P}^{\text{M}}) = -81.7$ ppm, $^2J(\text{P}^{\text{A}}, \text{P}^{\text{A}}) = 30$ Hz, $^2J(\text{P}^{\text{A}}, \text{P}^{\text{M}}) = 20$ Hz, $^2J(\text{P}^{\text{A}}, \text{P}^{\text{M}}) = 265$ Hz, $^2J(\text{P}^{\text{A}}, \text{P}^{\text{M}}) = 265$ Hz, $^2J(\text{P}^{\text{A}}, \text{P}^{\text{M}}) = 20$ Hz, $^2J(\text{P}^{\text{M}}, \text{P}^{\text{M}}) = 100$ Hz, $J(\text{P}^{\text{A}}, \text{Rh}^{\text{X}}) = 160$ Hz, $J(\text{P}^{\text{M}}, \text{Rh}^{\text{X}}) = 120$ Hz, $J(\text{P}^{\text{M}}, \text{Rh}^{\text{Y}}) = 100$ Hz; $^{11}\text{B}\{^1\text{H}\}$ RMN (96.3 MHz, $[\text{D}_6]\text{benzene}$, 25 °C): $\delta = -3.68$ ppm (s, BH); HRMS m/z calcd for $\text{C}_{57}\text{H}_{54}\text{BN}_6\text{P}_4\text{Rh}_2$ $[\text{M}+\text{H}]^+$ 1163.1567, found: 1163.1610 (error (mD) = -4.3); elemental analysis calcd (%) for $\text{C}_{57}\text{H}_{53}\text{N}_6\text{BP}_4\text{Rh}_2$ (1162.59): C 58.89, H 4.60, N 7.23; found: 56.93, H 4.80, N 7.99.

Reaction of $[\text{Rh}(\text{Tp})(\text{C}_2\text{H}_4)(\text{PPhPh}_2)]$ (2) with PMePh_2 : Methylidiphosphane (22 μL , 0.11 mmol) was added to a solution of $[\text{Rh}(\text{Tp})(\text{C}_2\text{H}_4)(\text{PPhPh}_2)]$ (2, 57.0 mg, 0.11 mmol) in toluene (5 mL). After stirring for 20 min, the solution was evaporated to 0.5 mL, layered with hexane (6 mL) and left steady overnight. The orange microcrystals that precipitated were separated by decantation, washed with cold hexane (1 \times 2 mL) and dried under vacuum. Yield: 60.8 mg (80%). IR(ATR): $\nu(\text{B-H})$ 2457 cm^{-1} (m), $\nu(\text{Rh-H})$ 2082 cm^{-1} (m); HRMS m/z calcd for $\text{C}_{34}\text{H}_{35}\text{BN}_6\text{P}_2\text{Rh}$ $[\text{M}+\text{H}]^+$ 703.1547, found: 703.1561 (error (mD) = -1.4); elemental analysis calcd (%) for $\text{C}_{34}\text{H}_{34}\text{N}_6\text{BP}_2\text{Rh}$ (702.34): C 58.14, H 4.88, N 11.97; found: C 57.41, H 4.89, N 12.22.

NMR data for $[\text{Rh}(\text{Tp})(\text{H})(\text{PMePh}_2)(\text{PPh}_2)]$ (8a, 70%): ^1H NMR (500.13 MHz, $[\text{D}_8]\text{toluene}$, 25 °C): $\delta = 8.05$ (t, $^3J(\text{H,H}) = ^3J(\text{H,P}) = 6.3$ Hz, 2H, PPh^{o1}), 7.62 (t, $^3J(\text{H,H}) = ^3J(\text{H,P}) = 7.6$ Hz, 2H, $\text{PMePh}_2^{\text{o1}}$), 7.59 (d, $^3J(\text{H,H}) = 1.9$ Hz, 1H, Pz^{B5}), 7.46 (brs, 1H, Pz^{B3}), 7.38 (d, $^3J(\text{H,H}) = 2.0$ Hz, 1H, Pz^{A5}), 7.26 (brt, $^3J(\text{H,H}) = ^3J(\text{H,P}) = 1.9$ Hz, 1H, Pz^{C5}), 7.18 (m, 2H, $\text{PMePh}_2^{\text{m1}}$), 7.10 (brs, 1H, Pz^{C3}), 7.03 (m, 6H, $\text{PPh}^{\text{(m+p1)}} + \text{PMePh}_2^{\text{o2}} + \text{PMePh}_2^{\text{p1}}$), 6.90 (td, $^3J(\text{H,H}) = 7.2$, $^4J(\text{H,H}) = 1.3$ Hz, 1H, $\text{PMePh}_2^{\text{p2}}$), 6.79 (m, 4H, $\text{PPh}^{\text{o2}} + \text{PMePh}_2^{\text{m2}}$), 6.67 (m, 3H, $\text{PPh}^{\text{(m+p2)}}$), 6.61 (d, $^3J(\text{H,H}) = 1.9$ Hz, 1H, Pz^{A3}), 5.91 (t, $^3J(\text{H,H}) = 2.0$ Hz, 1H, Pz^{B4}), 5.57 (t, $^3J(\text{H,H}) = 2.0$ Hz, 1H, Pz^{A4}), 5.52 (brt, $^3J(\text{H,H}) = 1.9$ Hz, 1H, Pz^{C4}), 4.62 (brd, $J(\text{H,B}) = 128.5$ Hz, 1H, HB), 1.94 (d, $J(\text{H,P}) = 9.2$ Hz, $J(\text{H,Rh}) = 1.4$ Hz, 3H, PMe), -14.90 ppm (ddd, $^2J(\text{H,P}) = 24.3$, 7.7 Hz, $J(\text{H,Rh}) = 15.0$ Hz, 1H, Rh–H); $^{31}\text{P}\{^1\text{H}\}$ NMR (202.5 MHz, $[\text{D}_8]\text{toluene}$, 25 °C): $\delta = 38.6$ (dd, $J(\text{P,Rh}) = 65$ Hz, $^2J(\text{P,P}) = 10$ Hz, 1P, PPh_2), 29.6 ppm (dd, $J(\text{P,Rh}) = 141$ Hz, $^2J(\text{P,P}) = 10$ Hz, 1P, PMePh_2); $^{11}\text{B}\{^1\text{H}\}$ NMR (128.4 MHz, $[\text{D}_8]\text{toluene}$, 25 °C): $\delta = -3.71$ ppm (s, BH).

Selected NMR resonances for $[\text{Rh}(\text{Tp})(\text{PMePh}_2)(\text{PPhPh}_2)]$ (8b, 30%): ^1H NMR (400.13 MHz, $[\text{D}_8]\text{toluene}$, 35 °C): $\delta = 5.38$ (dd, $^1J(\text{H,P}) = 352.0$, $^3J(\text{H,Rh}) = 18.1$ Hz, 1H, PPhPh_2), 1.58 ppm (d, $J(\text{H,P}) = 8.4$ Hz, 3H, PMePh_2); $^{31}\text{P}\{^1\text{H}\}$ NMR (161.3 MHz, $[\text{D}_8]\text{toluene}$, 80 °C): $\delta = 38.8$ (dd, $J(\text{P,Rh}) = 167$ Hz, $^2J(\text{P,P}) = 60$ Hz, 1P, PMePh_2), 28.7 ppm (dd, $J(\text{P,Rh}) = 176$ Hz, $^2J(\text{P,P}) = 60$ Hz, 1P, PPhPh_2); $^{11}\text{B}\{^1\text{H}\}$ NMR (128.4 MHz, $[\text{D}_8]\text{toluene}$, 25 °C): $\delta = -1.66$ ppm (s, BH).

$[\text{Rh}(\text{Tp})(\text{PMePh}_2)_2]$ (9): PMePh_2 (96.5 μL , 0.519 mmol) was added to a solution of $[\text{Rh}(\text{Tp})(\text{C}_2\text{H}_4)_2]$ (1, 96.5 mg, 0.259 mmol) in $[\text{D}_6]\text{benzene}$ (0.5 mL). The initial yellow solution immediately turned to dark yellow. After stirring for 30 min, the solution was concentrated to 0.5 mL and hexane (5 mL) was added. The yellow solid that precipitated was separated by decantation and washed with hexane (2 \times 5 mL). Yield: 126.4 mg (67%). IR(ATR): $\nu(\text{B-H})$ 2459 cm^{-1} (m). ^1H NMR (500.13 MHz, $[\text{D}_6]\text{benzene}$, 25 °C): $\delta = 7.84$ (brs, 3H, Pz), 7.65 (brs, 8H, PMePh_2), 6.99 (br, 15H, Pz + $\text{PMePh}_2^{\text{m+p}}$), 5.92 (brs, 3H, Pz), 1.29 ppm (td, $J(\text{H,P}) = 3.8$ Hz, $J(\text{H,Rh}) = 1.1$ Hz, 1H); $^{31}\text{P}\{^1\text{H}\}$ NMR (202.5 MHz, $[\text{D}_6]\text{benzene}$, 25 °C):

$\delta = 32.5$ ppm (d, $J(\text{P,Rh}) = 175$ Hz, PMePh_2); $^{11}\text{B}\{^1\text{H}\}$ NMR (160.5 MHz, $[\text{D}_6]\text{benzene}$, 25 °C): $\delta = -1.56$ ppm (s, BH); HRMS m/z calcd for $\text{C}_{35}\text{H}_{37}\text{BN}_6\text{P}_2\text{Rh}$ $[\text{M}+\text{H}]^+$ 716.1624, found: 716.1625 (error (mD) = 0.1); elemental analysis calcd (%) for $\text{C}_{35}\text{H}_{36}\text{N}_6\text{BP}_2\text{Rh}$ (716.38): C 58.68, H 5.07, N 11.73; found: C 58.61, H 4.95, N 11.17.

Reaction of $[\text{Rh}(\text{Tp})(\text{C}_2\text{H}_4)(\text{PPhPh}_2)]$ (2) with PPh_3 : An NMR tube was charged with equimolar amounts of complex 2 (15.9 mg, 0.03 mmol) and PPh_3 (7.9 mg, 0.03 mmol), $[\text{D}_8]\text{toluene}$ (0.5 mL) was added and the reaction was monitored by NMR. $^{31}\text{P}\{^1\text{H}\}$ NMR (161.3 MHz, $[\text{D}_8]\text{toluene}$, -60 °C) for $[\text{Rh}(\text{Tp})(\text{H})(\text{PPh}_3)(\text{PPh}_2)]$ (10a) $\delta = 46.6$ (dd, $J(\text{P,Rh}) = 141$, $^2J(\text{P,P}) = 12$ Hz, 1P, PPh_3), 41.1 ppm (dd, $J(\text{P,Rh}) = 68$, $^2J(\text{P,P}) = 12$ Hz, 1P, PPh_2); for $[\text{Rh}(\kappa^2\text{-Tp})(\text{PPh}_3)(\text{PPhPh}_2)]$ (10b-Tp-in) $\delta = 54.0$ (dd, $J(\text{P,Rh}) = 169$, $^2J(\text{P,P}) = 58$ Hz, 1P, PPh_3), 28.5 ppm (dd, $J(\text{P,Rh}) = 171$, $^2J(\text{P,P}) = 58$ Hz, 1P, PPhPh_2); for $[\text{Rh}(\kappa^2\text{-Tp})(\text{PPh}_3)(\text{PPhPh}_2)]$ (10b-Tp-out) $\delta = 54.6$ (dd, $J(\text{P,Rh}) = 168$, $^2J(\text{P,P}) = 55$ Hz, 1P, PPh_3), 32.0 ppm (dd, $J(\text{P,Rh}) = 171$, $^2J(\text{P,P}) = 55$ Hz, 1P, PPhPh_2); ^1H NMR (400.13 MHz, $[\text{D}_8]\text{toluene}$, 25 °C) selected resonances: $\delta = -14.45$ (ddd, $^2J(\text{H,P}) = 22.5$, $^2J(\text{H,P}) = 6.6$, $J(\text{H,Rh}) = 13.4$ Hz, 1H, Rh–H, 10a), 5.38 ppm (dd, $^1J(\text{H,P}) = 355.5$ Hz, $^3J(\text{H,Rh}) = 16.1$ Hz, 1H, PPhPh_2 , 10b); $^{11}\text{B}\{^1\text{H}\}$ NMR (128.4 MHz, $[\text{D}_8]\text{toluene}$, 25 °C): $\delta = -3.90$ (s, BH, 10a), -2.05 ppm (s, BH, 10b).

$[\text{Rh}(\text{Tp})(\text{IMes})(\text{PPhPh}_2)]$ (11): IMes (44.7 mg, 0.150 mmol) was added to a solution of $[\text{Rh}(\text{Tp})(\text{C}_2\text{H}_4)(\text{PPhPh}_2)]$ (2, 77.8 mg, 0.150 mmol) in toluene (5 mL). After stirring for 30 min, the solution was concentrated to 0.5 mL and layered with hexane (6 mL). The orange microcrystals that precipitated were separated by decantation, washed with hexane (2 mL) and dried under vacuum. Yield: 84 mg (71%). IR(ATR): $\nu(\text{B-H})$ 2433 cm^{-1} (m); ^1H NMR (400.13 MHz, $[\text{D}_6]\text{benzene}$, 25 °C): $\delta = 8.07$ (brs, 1H, Pz^{A3}), 7.91 (brs, 1H, Pz^{A5}), 7.84 (d, $^3J(\text{H,H}) = 2.4$ Hz, 1H, Pz^{C5}), 7.69 (d, $^3J(\text{H,H}) = 2.3$ Hz, 1H, Pz^{B5}), 7.43 (brs, 1H, Pz^{B3}), 7.38 (brt, $^3J(\text{H,H}) = ^3J(\text{H,P}) = 8.6$ Hz, 2H, HPPH^{o1}), 7.30 (m, 2H, HPPH^{o2}), 7.00 (brs, 4H, $\text{HPPH}^{\text{(m+p1+p2)}}$), 6.91 (t, $^3J(\text{H,H}) = 7.2$ Hz, HPPH^{m1}), 6.86 (s, 1H, Ar^{A}), 6.84 (s, 1H, Ar^{B}), 6.76 (d, $^3J(\text{H,H}) = 1.9$ Hz, 1H, Pz^{C3}), 6.50 (brt, $^3J(\text{H,H}) = 1.8$ Hz, Pz^{A4}), 6.43 (s, 1H, Ar^{B}), 6.39 (s, 1H, Ar^{A}), 6.23 (d, $^3J(\text{H,H}) = 1.9$ Hz, Im^1), 6.19 (d, $^3J(\text{H,H}) = 1.9$ Hz, Im^2), 5.95 (d, $J(\text{H,P}) = 332.5$ Hz, $^3J(\text{H,Rh}) = 3.3$ Hz, 1H, PPhPh_2), 5.87 (brt, 1H, Pz^{B4}), 5.47 (t, $^3J(\text{H,H}) = 2.2$ Hz, 1H, Pz^{C4}), 3.05 (s, 3H, Me^{A}), 2.23 (s, 3H, Me^{B}), 2.18 (s, 3H, Me^{C}), 2.04 (s, 3H, Me^{D}), 2.00 (s, 3H, Me^{E}), 1.59 ppm (s, 3H, Me^{F}); $^{31}\text{P}\{^1\text{H}\}$ NMR (162.0 MHz, $[\text{D}_6]\text{benzene}$, 25 °C): $\delta = 21.1$ (d, $J(\text{P,Rh}) = 195$ Hz, 1P, HPPH_2); $^{11}\text{B}\{^1\text{H}\}$ NMR (128.4 MHz, $[\text{D}_6]\text{benzene}$, 25 °C): $\delta = -2.55$ ppm (s, BH); HRMS m/z calcd for $\text{C}_{42}\text{H}_{45}\text{BN}_8\text{PrH}$ $[\text{M}]^+$ 806.2654, found: 806.2691 (error (mD) = -3.7); elemental analysis calcd (%) for $\text{C}_{42}\text{H}_{45}\text{N}_8\text{BPRh}$ (806.55): C 62.54, H 5.62, N 13.89; found: C 62.91, H 5.52, N 13.28.

$[\text{Rh}(\text{Tp})(\text{BzIm})(\text{PPhPh}_2)]$ (12) was prepared as described above for 10 starting from BzIm (12.8 mg, 0.088 mmol) and $[\text{Rh}(\text{Tp})(\text{C}_2\text{H}_4)(\text{PPhPh}_2)]$ (2, 46.4 mg, 0.088 mmol). Yield: 34.1 mg (60%). IR(ATR): $\nu(\text{B-H})$ 2468 cm^{-1} (m), ^1H NMR (400.13 MHz, $[\text{D}_8]\text{toluene}$, 65 °C): $\delta = 7.64$ (d, $^3J(\text{H,H}) = 2.1$ Hz, 3H, Pz^5), 7.36 (ddd, $^3J(\text{H,P}) = 11.1$, $^3J(\text{H,H}) = 7.8$, 1.7 Hz, 4H, HPPH^{o}), 7.26 (v br, 3H, Pz^3), 6.86 (m, 6H, $\text{HPPH}^{\text{m+p}}$), 6.81 (m, 2H) and 6.58 (m, 2H, A_2B_2 spin system, BzIm), 6.16 (dd, $J(\text{H,P}) = 322.7$, $^2J(\text{H,Rh}) = 1.1$ Hz, 1H, HPPH_2), 6.02 (brs, 3H, Pz^4), 3.59 ppm (s, 6H, Me); $^{31}\text{P}\{^1\text{H}\}$ NMR (162.0 MHz, $[\text{D}_8]\text{toluene}$, 65 °C): $\delta = 26.0$ (d, $J = 192$ Hz, PPhPh_2); $^{11}\text{B}\{^1\text{H}\}$ NMR (128.4 MHz, $[\text{D}_8]\text{toluene}$, -50 °C): $\delta = -1.93$ ppm (s, BH); HRMS m/z calcd for $\text{C}_{30}\text{H}_{30}\text{BN}_8\text{PrH}$ $[\text{M}-\text{H}]^+$ 647.1479, found: 647.1492 (error (mD) = -1.3); elemental analysis calcd (%) for $\text{C}_{30}\text{H}_{31}\text{N}_8\text{BPRh}$ (648.31): C 55.58, H 4.82, N 17.28; found: C 52.83, H 4.54, N 16.47.

$[\text{Rh}(\text{Tp})(\eta^1\text{-Et})(\kappa^{\text{C-P}}\text{-CH}_2\text{CH}_2\text{PPh}_2)]$ (13): An NMR tube was charged with $[\text{Rh}(\text{Tp})(\text{C}_2\text{H}_4)(\text{PPhPh}_2)]$ (2, 26.8 mg, 0.051 mmol) and benzene (0.6 mL) was added. The NMR tube was out under an ethylene atmosphere (6.0 bar) and the reaction mixture was heated at 60 °C

for 6 days to give a cloudy light-yellow solution. Then, toluene (2 mL) was added and the suspension was filtered off to remove small amounts of complex **3**. The filtrate was dried under vacuum, washed with hexane (2 × 0.5 mL) and dried under vacuum. Yield: 22.0 mg (78%). IR(ATR): $\nu(\text{B-H})$ 2460 cm^{-1} (m); $^1\text{H NMR}$ (500.13 MHz, $[\text{D}_6]$ benzene, 25 °C): δ = 7.74 (d, $^3J(\text{H,H})$ = 1.5 Hz, 1H, Pz^{A3}), 7.652 (d, $^3J(\text{H,H})$ = 2.2 Hz, 2H, Pz^{C3}), 7.651 (d, $^3J(\text{H,H})$ = 2.3 Hz, 1H, Pz^{A5}), 7.56 (dd, $^3J(\text{H,H})$ = 2.3 Hz, $^4J(\text{H,H})$ = 0.7 Hz, 1H, Pz^{B5}), 7.51 (ddd, $^3J(\text{H,P})$ = 9.9 Hz, $^3J(\text{H,H})$ = 7.5 Hz, $^4J(\text{H,H})$ = 1.7 Hz, 2H, PPh^{O1}), 7.49 (d, $^3J(\text{H,H})$ = 1.7 Hz, 1H, Pz^{C5}), 7.19 (dd, $^3J(\text{H,P})$ = 10.6 Hz, $^3J(\text{H,H})$ = 7.0 Hz, 2H, PPh^{O2}), 7.04 (m, 3H, $\text{PPh}^{\text{P+M1}}$), 6.87 (d, $^3J(\text{H,H})$ = 1.5 Hz, 1H, Pz^{B3}), 6.84 (t, $^3J(\text{H,H})$ = 7.5 Hz, 1H, PPh^{P2}), 6.71 (t, $^3J(\text{H,H})$ = 6.9 Hz, 2H, PPh^{M2}), 6.09 (t, $^3J(\text{H,H})$ = 2.1 Hz, 1H, Pz^{A4}), 5.94 (br, 1H, Pz^{C4}), 5.77 (t, $^3J(\text{H,H})$ = 2.1 Hz, 1H, Pz^{B4}), 3.95 (dtd, $^2J(\text{H,H})$ = 15.0 Hz, $^3J(\text{H,H})$ = $^2J(\text{H,P})$ = 10.9 Hz, $^3J(\text{H,H})$ = 6.4 Hz, 1H, H^{3A}), 3.64 (dtd, $^2J(\text{H,H})$ = 15.0 Hz, $^3J(\text{H,H})$ = $^2J(\text{H,P})$ = 10.6 Hz, $^3J(\text{H,H})$ = 2.1 Hz, 1H, H^{3B}), 2.23 (pd, $^3J(\text{H,H})$ = $^2J(\text{H,Rh})$ = 7.8 z, $^2J(\text{H,H})$ = 3.8 Hz, 1H, H^{1A}), 2.00 (pd, $^3J(\text{H,H})$ = $^2J(\text{H,Rh})$ = 7.7, $^2J(\text{H,H})$ = 3.8 Hz, 1H, H^{1A}), 1.72 (dddd, $^3J(\text{H,P})$ = 14.0 Hz, $^3J(\text{H,H})$ = 10.4 Hz, $^2J(\text{H,Rh})$ = 6.9 Hz, $^3J(\text{H,H})$ = 3.9 Hz, 1H, H^{2B}), 1.41 (dddd, $^3J(\text{H,P})$ = 13.3 Hz, $^3J(\text{H,H})$ = 10.8 Hz, $^2J(\text{H,Rh})$ = 7.8 Hz, $^3J(\text{H,H})$ = 2.7 Hz, 1H, H^{2A}), 1.00 ppm (t, $^3J(\text{H,H})$ = 7.8 Hz, 3H, Me); $^{31}\text{P}\{^1\text{H}\}$ NMR (202.5 MHz, $[\text{D}_6]$ benzene, 25 °C): δ = -36.1 ppm (d, $J(\text{P,Rh})$ = 122 Hz, 1P, PPh_2); $^{13}\text{C}\{^1\text{H}\}$ -APT NMR (125.8 MHz, $[\text{D}_6]$ benzene, 25 °C), selected resonances: δ = 36.0 (dd, $J(\text{C,P})$ = 32 Hz, $J(\text{C,Rh})$ = 4 Hz, C^3) 18.2 (Me), 11.8 (dd, $J(\text{C,Rh})$ = 24 Hz, $J(\text{C,P})$ = 11 Hz, C^1), -9.5 ppm (d, $J(\text{C,P})$ = 38 Hz, $J(\text{C,Rh})$ = 20 Hz, C^2); $^{11}\text{B}\{^1\text{H}\}$ NMR (160.5 MHz, $[\text{D}_6]$ benzene, 25 °C): δ = -3.52 ppm (s, BH); MS (m/z (%)): 558.2 (100) $[\text{M}]^+$; elemental analysis calcd (%) for $\text{C}_{25}\text{H}_{29}\text{N}_6\text{BPRh}$ (558.23): C 53.79, H 5.24, N 15.05; found: C 52.47, H 5.09, N 15.00.

[Rh(Tp)(H)(POPh₂)(PPh₂)] (14): Diphenylphosphane oxide (42.7 mg, 0.211 mmol) was added to a yellow solution of $[\text{Rh}(\text{Tp})(\text{C}_2\text{H}_4)(\text{HPPH}_2)]$ (**2**, 112.0 mg, 0.211 mmol) in toluene (3 mL) to produce an immediate color change to pale yellow. After stirring for 10 min, the solution was concentrated to 0.5 mL, layered with hexane (6 mL) and left steady for two days. The yellow microcrystals that precipitated were decanted, washed with cold hexane (1 × 2 mL) and dried under vacuum. Yield: 135.2 mg (91%). IR(ATR): $\nu(\text{B-H})$ 2464 cm^{-1} (m), $\nu(\text{Rh-H})$ 2114 cm^{-1} (m); $^1\text{H NMR}$ (500.13 MHz, $[\text{D}_6]$ benzene, 25 °C): δ = 8.52 (dd, $^3J(\text{H,P})$ = 10.7 Hz, $^3J(\text{H,H})$ = 7.1 Hz, 2H, POPh^{O1}), 8.36 (d, $^3J(\text{H,H})$ = 1.9 Hz, 1H, Pz^{B3}), 7.61 (m, 2H, PPh^{O1}), 7.58 (d, $^3J(\text{H,H})$ = 2.3 Hz, 1H, Pz^{B5}), 7.39 (d, $^3J(\text{H,H})$ = 2.6 Hz, 1H, Pz^{C5}), 7.35 (td, $^3J(\text{H,H})$ = 7.6 Hz, $^4J(\text{H,P})$ = 2.1 Hz, 2H, POPh^{M1}), 7.29 (d, $^3J(\text{H,H})$ = 2.2 Hz, 1H, Pz^{A5}), 7.22 (dtd, $^3J(\text{H,H})$ = 8.8, $^4J(\text{H,H})$ = 6.8 Hz, $^5J(\text{H,P})$ = 1.5 Hz, 1H, POPh^{P1}), 7.17 (dd, $J(\text{H,P})$ = 410.1 Hz, $^2J(\text{H,P})$ = 10.5 Hz, 1H, PPh_2), 7.09 (m, 4H, POPh^{O2} + PPh^{O2}), 6.99 (d, $^3J(\text{H,H})$ = 2.0 Hz, 1H, Pz^{A3}), 6.95 (m, 3H, $\text{PPh}^{\text{M+P1}}$), 6.88 (td, $^3J(\text{H,H})$ = 7.4 Hz, $^4J(\text{H,H})$ = 1.9 Hz, 1H, PPh^{P2}), 6.78 (m, 6H, $\text{POPh}^{\text{M+P2}}$ + PPh^{M2}), 6.77 (d, $^3J(\text{H,H})$ = 1.9 Hz, 1H, Pz^{C3}), 5.87 (t, $^3J(\text{H,H})$ = 2.1 Hz, 1H, Pz^{B4}), 5.62 (td, $^3J(\text{H,H})$ = 2.2 Hz, $^5J(\text{H,P})$ = 1.0 Hz, 1H, Pz^{C4}), 5.52 (td, $^3J(\text{H,H})$ = 1.8 Hz, $^5J(\text{H,P})$ = 0.9 Hz, 1H, Pz^{A4}), -13.74 (ddd, $^2J(\text{H,P})$ = 23.2 Hz, 20.4 Hz, $^1J(\text{H,Rh})$ = 16.0 Hz, 1H, Rh-H); $^{31}\text{P}\{^1\text{H}\}$ NMR (202.5 MHz, $[\text{D}_6]$ benzene, 25 °C): δ = 75.7 (dd, $^1J(\text{P,Rh})$ = 105 Hz, $^2J(\text{P,P})$ = 40 Hz, 1P, OPPh_2), 33.5 ppm (dd, $^1J(\text{P,Rh})$ = 140 Hz, $^2J(\text{P,P})$ = 40 Hz, 1P, PPh_2); $^{11}\text{B}\{^1\text{H}\}$ NMR (160.5 MHz, $[\text{D}_6]$ benzene, 25 °C): δ = -3.68 ppm (s, BH); HRMS m/z calcd for $\text{C}_{33}\text{H}_{33}\text{N}_6\text{BOP}_2\text{Rh}$ $[\text{M}+\text{H}]^+$ 705.1339, found 705.1332 (error (mD) = -0.7); elemental analysis calcd (%) for $\text{C}_{33}\text{H}_{32}\text{N}_6\text{BOP}_2\text{Rh}$ (704.31): C 56.28, H 4.58, N 11.93; found: 56.54, H 4.74, N 11.80.

[[[Tp](η^1 -Et)Rh(μ -OPPh₂)₂]] (15): A solution of OPPh_2 (61.3 mg, 0.303 mmol) in toluene (5 mL) was dropwise added over 45 min to a yellow solution of $[\text{Rh}(\text{Tp})(\text{C}_2\text{H}_4)]$ (**1**, 112.9 mg, 0.303 mmol) in toluene (7 mL). The resulting pale-yellow solution was evaporated to

dryness and the residue washed with acetone (3 × 1 mL) and dried under vacuum. Yield: 75.3 mg (46%). IR(ATR): $\nu(\text{B-H})$ 2485 cm^{-1} (m); $^1\text{H NMR}$ (400.13 MHz, $[\text{D}_6]$ benzene, 25 °C): δ = 8.02 (d, $^3J(\text{H,H})$ = 2.1 Hz, 1H, Pz^{A3}), 8.00 (m, 2H, POPh^{O1}), 7.57 (dd, $^3J(\text{H,H})$ = 2.3 Hz, $^4J(\text{H,H})$ = 0.6 Hz, 1H, Pz^{B5}), 7.46 (dd, $^3J(\text{H,H})$ = 2.5 Hz, $^4J(\text{H,H})$ = 0.8 Hz, 1H, Pz^{C5}), 7.38 (d, $^3J(\text{H,H})$ = 2.3 Hz, 1H, Pz^{A5}), 7.20 (t, $^3J(\text{H,H})$ = 7.1 Hz, 2H, POPh^{M1}), 7.16 (overlapped, 1H, Pz^{B3}), 7.14 (m, 3H, POPh^{O2} + POPh^{P1}), 6.99 (d, $^3J(\text{H,H})$ = 2.2 Hz, 1H, Pz^{C3}), 6.79 (ddd, $^3J(\text{H,H})$ = 8.8, 6.0 Hz, $^4J(\text{H,H})$ = 1.4 Hz, 1H, POPh^{P2}), 6.61 (t, $^3J(\text{H,H})$ = 7.3 Hz, 2H, POPh^{M2}), 5.75 (td, $^3J(\text{H,H})$ = 2.1 Hz, $^5J(\text{H,P})$ = 1.1 Hz, 1H, Pz^{A4}), 5.71 (t, $^3J(\text{H,H})$ = 2.3 Hz, 1H, Pz^{C4}), 5.67 (t, $^3J(\text{H,H})$ = 2.1 Hz, 1H, Pz^{B4}), 4.64 (p, $^3J(\text{H,H})$ = $^2J(\text{H,H})$ = 8.7 Hz, 1H, CH_2), 3.17 (h, $^3J(\text{H,H})$ = $^2J(\text{H,H})$ = $^3J(\text{H,P})$ = 8.7 Hz, 1H, CH_2), 1.15 ppm (t, $^3J(\text{H,H})$ = 7.5 Hz, 3H, Me); $^{31}\text{P}\{^1\text{H}\}$ NMR (162.0 MHz, $[\text{D}_6]$ benzene, 25 °C): δ = 91.4 ppm (m, AA' part of a AA'XX' spin system (A = ^{31}P , X = ^{103}Rh), OPPh_2); selected ^{13}C resonances from the ^1H - ^{13}C HSQC spectrum, δ = 20.1 (CH_2), 18.1 ppm (Me); $^{11}\text{B}\{^1\text{H}\}$ NMR (128.8 MHz, $[\text{D}_6]$ benzene, 25 °C): δ = -3.13 ppm (s, BH); HRMS m/z calcd for $\text{C}_{23}\text{H}_{25}\text{N}_6\text{BOP}_2\text{Rh}$ $[\text{M}+\text{H}]^+$ 547.1052, found: 547.1012 (error (mD) = 4.0); elemental analysis calcd (%) for $\text{C}_{23}\text{H}_{25}\text{N}_6\text{BOP}_2\text{Rh}$ (547.1052): C 49.94, H 4.72, N 15.16.

[Rh(Tp)(η^1 -R)(POPh₂)(POHPh₂)] (R = Et, **16 and **H**, **17**)**: Diphenylphosphane oxide (17.0 mg, 0.084 mmol) was added to a cloudy yellow suspension of $[[\text{Tp}(\eta^1\text{-Et})\text{Rh}(\mu\text{-OPPh}_2)_2]]$ (**15**, 46.0 mg, 0.042 mmol) in toluene (6 mL). After stirring for 14 hours at 60 °C, the light-yellow solution was evaporated, and the residue was crashed with hexane (5 mL). After that, the resulting white solid was washed with hexane (2 × 1 mL) and dried under vacuum. Yield: 60.9 mg (98%, ratio **16**:**17** = 2:1).

NMR data for $[\text{Rh}(\text{Tp})(\eta^1\text{-Et})(\text{POPh}_2)(\text{POHPh}_2)]$ (**16**, 66.6%): $^1\text{H NMR}$ (500.13 MHz, $[\text{D}_6]$ benzene, 25 °C): δ = 18.34 (brs, 1H, POH), 7.92 (dddd, $^3J(\text{H,H})$ = 7.9 Hz, $^3J(\text{H,P})$ = 5.7, $^4J(\text{H,H})$ = 3.7 Hz, $^4J(\text{H,H})$ = 1.6 Hz, 4H, POPh^{O1}), 7.55 (d, $^3J(\text{H,H})$ = 2.3 Hz, 4H, Pz^{A3A5}), 7.36 (d, $^3J(\text{H,H})$ = 2.3 Hz, 1H, Pz^{B5}), 7.12 (m, 4H, POPh^{M1}), 7.09 (m, 2H, POPh^{P1}), 6.91 (dddd, $^3J(\text{H,H})$ = 6.8 Hz, $^3J(\text{H,P})$ = 5.2, $^4J(\text{H,H})$ = 3.8 Hz, $^4J(\text{H,H})$ = 1.4 Hz, 4H, POPh^{O2}), 6.83 (m, 4H, POPh^{M2}), 6.75 (m, 2H, POPh^{P2}), 6.74 (d, $^3J(\text{H,H})$ = 2.3 Hz, 1H, Pz^{B3}), 5.84 (t, $^3J(\text{H,H})$ = 2.2 Hz, 1H, Pz^{A4}), 5.21 (t, $^3J(\text{H,H})$ = 2.1 Hz, 1H, Pz^{B4}), 2.22 (qtd, $^3J(\text{H,H})$ = 7.5 Hz, $^3J(\text{H,P})$ = 4.1 Hz, $^2J(\text{H,Rh})$ = 1.9 Hz, 2H, CH_2), 0.52 ppm (t, $^3J(\text{H,H})$ = 7.5 Hz, 3H, Me); $^{31}\text{P}\{^1\text{H}\}$ NMR (202.5 MHz, $[\text{D}_6]$ benzene, 25 °C): δ = 88.2 ppm (d, $J(\text{P,Rh})$ = 140 Hz, 2P); $^{11}\text{B}\{^1\text{H}\}$ NMR (160.5 MHz, $[\text{D}_6]$ benzene, 25 °C): δ = -4.24 ppm (s, BH).

NMR data for $[\text{Rh}(\text{Tp})(\text{H})(\text{POPh}_2)(\text{POHPh}_2)]$ (**17**, 33.3%): $^1\text{H NMR}$ (500.13 MHz, $[\text{D}_6]$ benzene, 25 °C): δ = 18.34 (brs, 1H, POH), 8.18 (dddd, $^3J(\text{H,H})$ = 7.1 Hz, $^3J(\text{H,P})$ = 5.9, $^4J(\text{H,H})$ = 3.9 Hz, $^4J(\text{H,H})$ = 2.1 Hz, 4H, POPh^{O1}), 7.42 (d, $^3J(\text{H,H})$ = 2.3 Hz, 1H, Pz^{B5}), 7.33 (d, $^3J(\text{H,H})$ = 2.5 Hz, 1H, Pz^{A5}), 7.12 (m, 4H, POPh^{O2}), 7.10 (m, 1H, Pz^{B3}), 7.09 (m, 4H, POPh^{M1}), 7.08 (m, 2H, POPh^{P1}), 6.80 (m, 2H, POPh^{P2}), 6.76 (m, 4H, POPh^{M2}), 6.68 (d, $^3J(\text{H,H})$ = 2.0 Hz, 1H, Pz^{A3}), 5.54 (t, $^3J(\text{H,H})$ = 2.3 Hz, 1H, Pz^{A4}), 5.52 (t, $^3J(\text{H,H})$ = 2.2 Hz, 1H, Pz^{B4}), -12.99 ppm (td, $^2J(\text{H,P})$ = 21.7 Hz, $J(\text{H,Rh})$ = 16.7 Hz, 1H, Rh-H); $^{31}\text{P}\{^1\text{H}\}$ NMR (202.5 MHz, $[\text{D}_6]$ benzene, 25 °C): δ = 97.3 ppm (d, $J(\text{P,Rh})$ = 128 Hz, 2P); $^{11}\text{B}\{^1\text{H}\}$ NMR (160.5 MHz, $[\text{D}_6]$ benzene, 25 °C): δ = -4.24 ppm (s, BH).

DFT geometry optimizations

The DFT geometry optimizations and thermochemical calculations were carried out with the Gaussian 09 program package,^[51] using the B3LYP-D3 hybrid functional.^[52] Geometry optimizations were performed in the gas phase with the LanL2TZ(f) effective core potential basis set for the metal atoms, and the 6-311G(d,p) basis set for the remaining ones.

Profiles for reactions in Figures 8–10 were computed with the Turbomole program^[53] coupled to the PQS Baker optimizer^[54] by the BOpt package.^[55] Geometries were fully optimized as minima or transition states using the BP86 functional,^[56] the Turbomole def2-TZVP basis set^[57] and a small grid size (m4). To reduce computation time, the resolution-of-identity (rI) approximation^[58] was applied. Grimme's dispersion corrections (version D3, disp3, 'zero damping') were applied to include Van der Waals interactions.^[52d]

X-ray diffraction studies on complexes [(Tp)(H)Rh(μ -PPh₂)₂Rh(PHPh₂)₂] 0.5H₂O (7·0.5H₂O), [Rh(Tp)(IMes)(PHPh₂)₂] (11) and [Rh(Tp)(H)(POPh₂)(PHPh₂)₂] (14)

Intensity measurements were collected with a Bruker Smart Apex-III (7 and 11) or a Bruker Smart Apex (14) diffractometers, with graphite-monochromated MoK α radiation at 100 K (ω scans of 0.3°). A semi-empirical absorption correction was applied to the data set with the multi-scan^[59] methods. The structures were solved by direct methods with SHELXS-2013^[60] (7 and 14) or SHELXT-2014^[61] (11) and refined by full-matrix least-squares on F^2 with the program SHELXL-2016,^[62] in the WINGX^[63] package. In the 24.7(14)% of the crystal of 14 the phosphanido and the phosphane oxide ligands are swapped. All non-hydrogen atoms were refined with anisotropic displacement parameters, and their hydrogen atoms were geometrically calculated and refined by the riding mode, including the isotropic displacement parameters. The hydride ligands were located in difference-Fourier maps and refined with a geometrical restraint (DFIX card). The hydrogens bonded to phosphorus (7 and 11) or boron atoms (7) were also located in a difference-Fourier map and refined with some degree of freedom. Hydrogen atoms of the water solvent (7) were not included in the model. For selected crystallographic data see the Supporting Information.

CCDC 1949932 (7·0.5H₂O), 1949933 (11), and 1949934 (14) contain the supplementary crystallographic data for this paper. These data are provided free of charge by The Cambridge Crystallographic Data Centre.

Acknowledgements

The generous financial support from AEI/FEDER, UE (CTQ2017-83421-P, C.T.), Gobierno de Aragón/FEDER (GA/FEDER, Inorganic Molecular Architecture Group E08_17R; C.T.) and the Netherlands Organization for Scientific Research (NWO) (TOP Grant 716.015.001, B.dB) is gratefully acknowledged. V.V. thanks MINECO/FEDER for an FPI fellowship. The 'Centro de Supercomputación de Galicia (CESGA)' is also gratefully acknowledged for generous allocation of time.

Conflict of interest

The authors declare no conflict of interest.

Keywords: insertion • oxidative addition • P–H activation • rhodaphosphacyclobutane • rhodium

- [1] See for example: a) S. Bezenine-Lafollée, R. Gil, D. Prim, J. Hannedouche, *Molecules* **2017**, *22*, 1901; b) C. A. Bange, R. Waterman, *Chem. Eur. J.* **2016**, *22*, 12598–12605; c) A. A. Trifonov, I. V. Basalov, A. A. Kissel, *Dalton Trans.* **2016**, *45*, 19172–19193; d) V. Koshti, S. Gaikwad, S. H. Chikkali, *Coord. Chem. Rev.* **2014**, *265*, 52–73; e) P. E. Sues, A. J. Lough,

- R. H. Morris, *J. Am. Chem. Soc.* **2014**, *136*, 4746–4760, and references therein; f) L. Rosenberg, *ACS Catal.* **2013**, *3*, 2845–2855; g) R. Waterman, *Chem. Soc. Rev.* **2013**, *42*, 5629–5641; h) *Hydrofunctionalization, Topics in Organometallic Chemistry, Vol. 43* (Eds.: V. P. Ananikov, I. P. Beletskaya), Springer, Heidelberg, **2013**, pp. 1–20; i) E. M. Leitao, T. Jurca, I. Manners, *Nat. Chem.* **2013**, *5*, 817–829; j) R. Waterman, *Curr. Org. Chem.* **2012**, *16*, 1313–1331; k) D. S. Glueck, *Top. Organomet. Chem.* **2010**, *31*, 65–100; l) S. Greenberg, D. W. Stephan, *Chem. Soc. Rev.* **2008**, *37*, 1482–1489; m) T. J. Clark, K. Lee, I. Manners, *Chem. Eur. J.* **2006**, *12*, 8634–8648; n) C. A. Jaska, A. Bartole-Scott, I. Manners, *Dalton Trans.* **2003**, 4015–4021.
- [2] a) R. Waterman, *Dalton Trans.* **2009**, 18–26; b) D. S. Glueck, *Dalton Trans.* **2008**, 5276–5286.
- [3] T. Chen, C.-Q. Zhao, L.-B. Han, *J. Am. Chem. Soc.* **2018**, *140*, 3139–3155.
- [4] Y. Xu, Z. Yang, B. Ding, D. Liu, Y. Liu, M. Sugiya, T. Imamoto, W. Zhang, *Tetrahedron* **2015**, *71*, 6832–6839.
- [5] S. K. Gibbons, Z. Xu, R. P. Hughes, D. S. Glueck, A. L. Rheingold, *Organometallics* **2018**, *37*, 2159–2166.
- [6] R. L. Webster, *Inorganics* **2018**, *6*, 120.
- [7] a) A. K. King, K. J. Gallagher, M. F. Mahon, R. L. Webster, *Chem. Eur. J.* **2017**, *23*, 9039–9043; b) M. Espinal-Viguri, A. K. King, J. P. Lowe, M. F. Mahon, R. L. Webster, *ACS Catal.* **2016**, *6*, 7892–7897; c) A. K. King, A. Buchard, M. F. Mahon, R. L. Webster, *Chem. Eur. J.* **2015**, *21*, 15960–15963.
- [8] a) A. N. Selikhov, T. V. Mahrova, A. V. Cherkasov, G. K. Fukin, E. Kirillov, C. A. Lamsfus, L. Maron, A. A. Trifonov, *Organometallics* **2016**, *35*, 2401–2409; b) W. Ma, L. Xu, W.-X. Zhang, Z. Xi, *New J. Chem.* **2015**, *39*, 7649–7655; c) A. C. Behrle, L. Castro, L. Maron, R. Walensky, *J. Am. Chem. Soc.* **2015**, *137*, 14846–14849; d) A. C. Behrle, J. A. R. Schmidt, *Organometallics* **2013**, *32*, 1141–1149; e) W.-X. Zhang, M. Nishiura, T. Mashiko, Z. Hou, *Chem. Eur. J.* **2008**, *14*, 2167–2179; f) M. R. Douglass, T. J. Marks, *J. Am. Chem. Soc.* **2000**, *122*, 1824–1825.
- [9] a) J. Yuan, H. Hu, C. Cui, *Chem. Eur. J.* **2016**, *22*, 5778–5785; b) X. Gu, L. Zhang, X. Zhu, S. Wang, S. Zhou, Y. Wei, G. Zhang, X. Mu, Z. Huang, D. Hong, F. Zhang, *Organometallics* **2015**, *34*, 4553–4559.
- [10] a) R. Waterman, *Organometallics* **2007**, *26*, 2492–2494; b) M. Driess, J. Aust, K. Merz, *Eur. J. Inorg. Chem.* **2002**, 2961–2964.
- [11] J. Li, C. A. Lamsfus, C. Song, J. Liu, G. Fan, L. Maron, C. Cui, *ChemCatChem* **2017**, *9*, 1368–1372.
- [12] a) K.-S. Feichtner, V. H. Gessner, *Chem. Commun.* **2018**, *54*, 6540–6553; b) J. Weismann, L. T. Scharf, V. H. Gessner, *Organometallics* **2016**, *35*, 2507–2515.
- [13] a) X. Qi, H. Zhao, H. Sun, X. Li, O. Fuhr, D. Fenske, *New J. Chem.* **2018**, *42*, 16583–16590; b) C. Martin, S. Mallet-Ladeira, K. Miqueu, G. Bouhadir, D. Bourissou, *Organometallics* **2014**, *33*, 571–577; c) E. J. Derrah, C. Martin, S. Mallet-Ladeira, K. Miqueu, G. Bouhadir, D. Bourissou, *Organometallics* **2013**, *32*, 1121–1128.
- [14] Y. Gloaguen, W. Jacobs, B. de Bruin, M. Lutz, J. I. van der Vlugt, *Inorg. Chem.* **2013**, *52*, 1682–1684.
- [15] R. A. Schunn, *Inorg. Chem.* **1973**, *12*, 1573–1579.
- [16] a) E. A. V. Ebsworth, R. A. Mayo, *J. Chem. Soc. Dalton Trans.* **1988**, 477–484; b) E. A. V. Ebsworth, R. O. Gould, R. A. Mayo, M. Walkinshaw, *J. Chem. Soc. Dalton Trans.* **1987**, 2831–2838; c) E. A. V. Ebsworth, R. Mayo, *Angew. Chem. Int. Ed. Engl.* **1985**, *24*, 68–70; *Angew. Chem.* **1985**, *97*, 65–66.
- [17] a) A. L. Serrano, M. A. Casado, M. A. Ciriano, B. de Bruin, J. A. López, C. Tejel, *Inorg. Chem.* **2016**, *55*, 828–839; b) I. Mena, M. A. Casado, V. Polo, P. García-Orduña, F. J. Lahoz, L. A. Oro, *Dalton Trans.* **2014**, *43*, 1609–1619.
- [18] a) I. Kovacic, D. K. Wicht, N. S. Grewal, D. S. Glueck, C. D. Incarvito, I. A. Guzei, A. L. Rheingold, *Organometallics* **2000**, *19*, 950–953; b) I. V. Kourkine, M. D. Sargent, D. S. Glueck, *Organometallics* **1998**, *17*, 125–127; c) D. K. Wicht, I. V. Kourkine, B. M. Lew, J. M. Nthenge, D. S. Glueck, *J. Am. Chem. Soc.* **1997**, *119*, 5039–5040.
- [19] Y. S. Ganushevich, V. A. Miluykov, F. M. Polyancev, S. K. Latypov, P. Lönnecke, E. Hey-Hawkins, D. G. Yakhvarov, O. G. Sinyashin, *Organometallics* **2013**, *32*, 3914–3919.
- [20] G. Bai, P. Wei, A. K. Das, D. W. Stephan, *Dalton Trans.* **2006**, 1141–1146.
- [21] a) M. Itazaki, Y. Nishihara, K. Osakada, *Organometallics* **2004**, *23*, 1610–1621.

- [22] D. Wang, Q. Chen, X. Leng, L. Deng, *Inorg. Chem.* **2018**, *57*, 15600–15609.
- [23] J. B. Bonanno, P. T. Wolczanski, E. B. Lobkovsky, *J. Am. Chem. Soc.* **1994**, *116*, 11159–11160.
- [24] R. T. Baker, J. C. Calabrese, R. L. Harlow, I. D. Williams, *Organometallics* **1993**, *12*, 830–841.
- [25] L. D. Field, N. G. Jones, P. Turner, *J. Organomet. Chem.* **1998**, *571*, 195–199.
- [26] L.-B. Han, T. D. Tilley, *J. Am. Chem. Soc.* **2006**, *128*, 13698–13699.
- [27] V. P. W. Böhm, M. Brookhart, *Angew. Chem. Int. Ed.* **2001**, *40*, 4694–4696; *Angew. Chem.* **2001**, *113*, 4832–4834.
- [28] U. Fischbach, M. Trincado, H. Grützmacher, *Dalton Trans.* **2017**, *46*, 3443–3448.
- [29] A. M. Geer, A. L. Serrano, B. de Bruin, M. A. Ciriano, C. Tejel, *Angew. Chem. Int. Ed.* **2015**, *54*, 472–475; *Angew. Chem.* **2015**, *127*, 482–485.
- [30] a) R. Shimogawa, Y. Tsurumaki, T. Kuzutani, T. Takao, *Organometallics* **2018**, *37*, 290–293; b) G. Luo, Y. Luo, Z. Hou, *Organometallics* **2017**, *36*, 4611–4619; c) M. P. Shaver, M. D. Fryzuk, *Organometallics* **2005**, *24*, 1419–1427.
- [31] W. C. Fultz, A. L. Rheingold, P. E. Kretrler, D. W. Meek, *Inorg. Chem.* **1983**, *22*, 860–863.
- [32] See, for example: a) D. O. Downing, P. Zavalij, B. W. Eichhorn, *Inorg. Chim. Acta* **2011**, *375*, 329–332; b) C. Tejel, M. Sommovigo, M. A. Ciriano, J. A. López, F. J. Lahoz, L. A. Oro, *Angew. Chem. Int. Ed.* **2000**, *39*, 2336–2339; *Angew. Chem.* **2000**, *112*, 2426–2429; c) K. Wang, T. J. Emge, A. S. Goldman, *Inorg. Chim. Acta* **1997**, *255*, 395–398; d) A. M. Arif, R. A. Jones, M. H. Seeberger, B. R. Whittlesey, T. C. Wright, *Inorg. Chem.* **1986**, *25*, 3943–3949; e) E. W. Burkhardt, W. C. Mercer, G. L. Geoffroy, *Inorg. Chem.* **1984**, *23*, 1779–1782; f) P. E. Kreter, D. W. Meek, *Inorg. Chem.* **1983**, *22*, 319–326; g) R. A. Jones, T. C. Wright, J. L. Atwood, W. E. Hunter, *Organometallics* **1983**, *2*, 470–472.
- [33] a) J. Kadis, Y. K. Shin, J. I. Dulebohn, D. L. Ward, D. G. Nocera, *Inorg. Chem.* **1996**, *35*, 811–817; b) J. I. Dulebohn, D. L. Ward, D. G. Nocera, *J. Am. Chem. Soc.* **1988**, *110*, 4054–4056.
- [34] a) D. W. Meek, P. E. Kreter, G. G. Christoph, *J. Organomet. Chem.* **1982**, *231*, C53–C58; b) S. K. Kang, T. A. Albright, T. C. Wright, R. A. Jones, *Organometallics* **1985**, *4*, 666–675.
- [35] Complexes [Rh(acac)(L)(CO)] were prepared in situ by addition of the appropriate ligand to solutions of [Rh(acac)(CO)₂] in toluene. The related [Rh(Tp)(L)(CO)] complexes were not used in this study since the κ^2 - κ^3 isomerism complicate the IR spectra.
- [36] a) D. G. Gusev, *Organometallics* **2009**, *28*, 763–770; b) D. G. Gusev, *Organometallics* **2009**, *28*, 6458–6461.
- [37] J. A. Billbrey, A. H. Kazez, J. Locklin, W. D. Allen, *J. Comput. Chem.* **2013**, *34*, 1189–1197.
- [38] C. Slugovc, I. Padilla-Martínez, S. Sirol, E. Carmona, *Coord. Chem. Rev.* **2001**, *213*, 129–157.
- [39] M. Paneque, P. J. Pérez, A. Pizzano, M. L. Poveda, S. Taboada, M. Trujillo, E. Carmona, *Organometallics* **1999**, *18*, 4304–4310.
- [40] P. E. Garrou, *Chem. Rev.* **1981**, *81*, 229–266.
- [41] a) K. M. E. Burton, D. A. Pantazis, R. G. Belli, R. McDonald, L. Rosenberg, *Organometallics* **2016**, *35*, 3970–3980; b) R. G. Belli, K. M. E. Burton, S. A. Ruff, R. McDonald, L. Rosenberg, *Organometallics* **2015**, *34*, 5637–5646; c) E. J. Derrah, R. McDonald, L. Rosenberg, *Chem. Commun.* **2010**, *46*, 4592–4594; d) E. J. Derrah, D. A. Pantazis, R. McDonald, L. Rosenberg, *Angew. Chem. Int. Ed.* **2010**, *49*, 3367–3370; *Angew. Chem.* **2010**, *122*, 3439–3442.
- [42] H. Geissler, P. Gross, B. Guckes, New pallada-phospha-cyclobutane compounds obtained by reacting special triorganyl-phosphane compounds with palladium salts palladium complexes or alkali palladate salts in organic, DE 19647584-A1, **1998**.
- [43] a) E. Igartúa-Nieves, A. J. Rivera-Brown, J. E. Cortés-Figueroa, *Inorg. Chem. Commun.* **2012**, *21*, 43–46; b) C. Cao, T. Wang, B. O. Patrick, J. A. Love, *Organometallics* **2006**, *25*, 1321–1324; c) M. A. Bennett, S. K. Bhargava, M. Ke, A. C. Willis, *J. Chem. Soc. Dalton Trans.* **2000**, 3537–3545.
- [44] R. Waterman, G. L. Hillhouse, *J. Am. Chem. Soc.* **2003**, *125*, 13350–13351.
- [45] For a first order reaction ($\ln \frac{[A]_t}{[A]_0} = -kt$) reaching 99% conversion in six days, the rate constant k is approximately $8.9 \times 10^{-6} \text{ s}^{-1}$, which translates to a free energy barrier ΔG^\ddagger of approximately $+27.3 \text{ kcal mol}^{-1}$ by using the Eyring–Polanyi equation ($k = \frac{k_B T}{h} e^{-\frac{\Delta G^\ddagger}{RT}}$ with k_B = Boltzmann constant, R = gas constant, h = Planck constant, and assuming a transmission coefficient of 1).
- [46] a) V. P. Ananikov, A. V. Makarov, I. P. Beletskaya, *Chem. Eur. J.* **2011**, *17*, 12623–12630; b) V. P. Ananikov, I. P. Beletskaya, *Chem. Asian J.* **2011**, *6*, 1423–1430.
- [47] $2.6 \text{ kcal mol}^{-1}$ (DFT gas phase): A. Christiansen, C. Li, M. Garland, D. Selent, R. Ludwig, A. Spannenberg, W. Baumann, R. Franke, A. Börner, *Eur. J. Org. Chem.* **2010**, 2733–2741.
- [48] J. A. López, private communication.
- [49] A. M. Geer, J. A. López, M. A. Ciriano, C. Tejel, *Organometallics* **2016**, *35*, 799–808, and references therein.
- [50] S. Trofimenko, *J. Am. Chem. Soc.* **1969**, *91*, 588–595.
- [51] See the Supporting Information for a complete reference.
- [52] a) C. Lee, W. Yang, R. G. Parr, *Phys. Rev. B* **1988**, *37*, 785–789; b) A. D. Becke, *J. Chem. Phys.* **1993**, *98*, 1372–1377; c) A. D. Becke, *J. Chem. Phys.* **1993**, *98*, 5648–5652; d) S. Grimme, J. Antony, S. Ehrlich, H. Krieg, *J. Chem. Phys.* **2010**, *132*, 154104.
- [53] University of Karlsruhe and Forschungszentrum Karlsruhe GmbH. *TURBOMOLE V7.3.1*; TURBOMOLE GmbH, **2018**.
- [54] J. Baker, *J. Comput. Chem.* **1986**, *7*, 385.
- [55] P. H. M. Budzelaar, *J. Comput. Chem.* **2007**, *28*, 2226.
- [56] a) J. P. Perdew, *Phys. Rev. B: Condens. Matter Mater. Phys.* **1986**, *33*, 8822; b) A. D. Becke, *Phys. Rev. A: At., Mol. Opt. Phys.* **1988**, *38*, 3098.
- [57] F. Weigend, R. Ahlrichs, *Phys. Chem. Chem. Phys.* **2005**, *7*, 3297.
- [58] a) K. Eichkorn, F. Weigend, O. Treutler, R. Ahlrichs, *Theor. Chem. Acc.* **1997**, *97*, 119; b) K. Eichkorn, O. Treutler, H. Öhm, M. Häser, R. Ahlrichs, *Chem. Phys. Lett.* **1995**, *240*, 283; c) F. Weigend, *Phys. Chem. Chem. Phys.* **2006**, *8*, 1057.
- [59] G. M. Sheldrick, SADABS, Bruker AXS, Madison, WI (USA), **1997**.
- [60] G. M. Sheldrick, *Acta Crystallogr. Sect. A* **2008**, *64*, 112–122.
- [61] G. M. Sheldrick, *Acta Crystallogr. Sect. A* **2015**, *71*, 3–8.
- [62] G. M. Sheldrick, *Acta Crystallogr. Sect. C* **2015**, *71*, 3–8.
- [63] L. J. Farrugia, *J. Appl. Crystallogr.* **2012**, *45*, 849–854.

Manuscript received: August 30, 2019

Revised manuscript received: October 3, 2019

Accepted manuscript online: October 4, 2019

Version of record online: November 8, 2019